Spring 2014

Effect Of Multivalent Ions On The Swelling And Mechanical Behavior Of Superabsorbent Polymers (Saps) For Mitigation Of Mortar Autogenous Shrinkage

Qian Zhu
Purdue University

Graduate School ETD Form 9
(Revised 01/14)

PURDUE UNIVERSITY
GRADUATE SCHOOL
Thesis/Dissertation Acceptance

This is to certify that the thesis/dissertation prepared

By Qian Zhu

Entitled
Effect of Multivalent Ions on the Swelling and Mechanical Behavior of Superabsorbent Polymers (SAPs) for Mitigation of Mortar Autogenous Shrinkage

For the degree of Master of Science in Materials Engineering

Is approved by the final examining committee:

Kendra A. Erk

W. Jason Weiss

John A. Howarter

To the best of my knowledge and as understood by the student in the *Thesis/Dissertation Agreement. Publication Delay, and Certification/Disclaimer (Graduate School Form 32)*, this thesis/dissertation adheres to the provisions of Purdue University's "Policy on Integrity in Research" and the use of copyrighted material.

Kendra A. Erk

Approved by Major Professor(s): _____

Approved by: David Bahr 04/18/2014

Head of the Department Graduate Program Date

EFFECT OF MULTIVALENT IONS ON THE SWELLING AND MECHANICAL BEHAVIOR OF SUPERABSORBENT POLYMERS (SAPS) FOR MITIGATION OF MORTAR AUTOGENOUS SHRINKAGE

A Thesis

Submitted to the Faculty

of

Purdue University

by

Qian Zhu

In Partial Fulfillment of the

Requirements for the Degree

of

Master of Science in Materials Engineering

May 2014

Purdue University

West Lafayette, Indiana

I dedicate my thesis to my loving parents who have always stood by my side.

ACKNOWLEDGEMENTS

Foremost I would like to express my sincere gratitude to my research advisor Professor Kendra A. Erk for her continuous guidance and encouragement throughout the program. Her knowledge and enthusiasm inspired me to be a better researcher. Besides, I would like to thank Professor John Howarter and Professor W. Jason Weiss for their valuable advice. Many thanks also go to Christopher Barney, Timothy Barrett, Albert Miller for their help of collecting data.

TABLE OF CONTENTS

Page

LIST OF TABLES

LIST OF FIGURES

Figure Page

Figure Page

ABSTRACT

Zhu, Qian. M.S.M.S.E., Purdue University, May 2014. Effect of Multivalent Ions on the Swelling and Mechanical Behavior of Superabsorbent Polymers (SAPs) for Mitigation of Mortar Autogenous Shrinkage. Major Professor: Kendra Erk.

The chemical and physical structure-property relationships of model superabsorbent polymer (SAP) hydrogels were characterized with respect to swelling behavior and mechanical properties in different ionic solutions (Na^{+}, Ca^{2+}, and Al^{3+}). The model hydrogels were composed of poly(sodium acrylate-acrylamide) (PANa-PAM) copolymer with varying concentrations of PANa (0, 17, 33, 67, and 83 wt.%) and covalent crosslinking densities of 1, 1.5, and 2 wt.%. By synthesizing the hydrogels in-house, systems with independently tunable amounts of covalent crosslinking and anionic functional groups were created, allowing for the relative effects of covalent and ionic crosslinking on the properties of the hydrogels to be directly quantified. It was found that the presence of Ca^{2+} and Al^{3+} in the absorbed fluid significantly decreased the swelling capacity and altered the swelling kinetics of the PANa-PAM hydrogels. The presence of Al^{3+} in solution resulted in the unexpected formation of a mechanically stiff barrier layer at the hydrogel's surface, which hindered the release of fluid and caused the overall elastic modulus of the hydrogel to increase from O(10 kPa) for hydrogels immersed in Ca^{2+} solutions to O(100 kPa) for hydrogels immersed in Al^{3+} solutions.

Tensile tests performed on isolated specimens of the stiff barrier layer yielded elastic moduli in the *O*(50-100 MPa) range. Further experiments proved that PANa-PAM hydrogels are effective to keep mortar internal relative humidity at high value (~98%) during setting and also PANa-PAM decreased the autogenous shrinkage of mortar to less than 50 microstrain while plain mortar showed 350 microstrain.

CHAPTER 1. INTRODUCTION

1.1 Research Motivation

Superabsorbent polymers (SAP particles) that serve as internal water supply to mitigate the autogenous shrinkage of high performance concrete (HPC) has been studied for 15 years since Jensen first brought up this research area in the beginning of 21st century.[1,2] The effectiveness of SAP particles on decreasing autogenous shrinkage of cement paste, mortar and HCP is widely known.[2,3,4,5] In previous studies, the amount of SAP particles, the size of SAP particles and the water/cement has been reported as the authors discussed the effect of SAP particles on mitigating the autogenous shrinkage of HPC. However, the chemical structures of the particles are seldom reported.

It is well known in polymer science that the chemical structures and the properties of the swelling medium will affect the swelling behavior of SAP particles which is very important for SAP particles serving as the internal curing agent but rarely studied in civil engineering. Multiple factors that influence the absorbency of SAP particles have been reported such as the crosslinking density, amount of initiator, ionic/non-ionic monomer ratios, pH value of swelling media, different ions and ionic strength of swelling media, temperature of swelling media,etc.[6,7,8,9,10] Among those parameters, the type of ions in

the swelling media should receive the most attention especially for the application of SAP particles in concrete since the swelling response of SAP particles in the presence of mono-valent ions (Na^+, K^+) and multi-valent ions (Ca^{2+}) which is released during the hydration process of concrete is very different. It's been found that the absorbency of SAP particles in multi-valent ion (Ca^{2+}) solutions is much lower than that in mono-valent ions (Na^+, K^+) solutions. [3,9,11] As a result, there is a critical need to understand the relationship between the chemical structures of SAP particles and their swelling behavior in multi-valent ion solutions, the primary requirement for predicting the swelling response of SAP particles in concrete.

While some research efforts have focused on quantifying the effect of Ca^{2+} on swelling behavior, the exact relationship between ionic sensitivity and the physical and chemical molecular structures of SAP particles has not been directly investigated.[3] This inspired us to synthesize SP systems with well-defined chemical structures and study the relationship between the molecular structures of SAP particles and their swelling response to different ion solutions. By studying that, we hope to provide guidance for customizing the SAP particles for concrete application. The majority of this work was recently accepted for publication by Materials & Structures (2014): "Effect of ionic crosslinking on the swelling and mechanical response of model superabsorbent polymer hydrogels for internally cured concrete", by Q. Zhu, C.W. Barney, and K.A. Erk .

1.2 Thesis Scope and Objectives

In the present work,[12] a series of random poly(sodium acrylate-acrylamide) copolymer (PANa-PAM) hydrogels with systematically varied concentrations of covalent crosslinks and anionic groups within the polymer network were synthesized. The hydrogels were immersed in aqueous fluids containing different ionic concentrations and valency, including Na^+, Ca^{2+}, and Al^{3+}(which is also present in cement pore solution[13]). The swelling response and mechanical properties of the hydrogels were measured, and the experimental results were related to the physical and chemical structures of the hydrogel. Finally, we mixed two PANa-PAM hydrogels with different chemical structures in mortar and evaluated their ability to mitigate the autogenous shrinkage of the mortar.

In this work, we hope to answer the following questions:

1) How will the swelling response of the synthesized PANa-PAM hydrogels be affected in deioinzed water, Na^+, Ca^{2+}, and Al^{3+} solutions?

2) How will the chemical structures of the PANa-PAM hydrogels affect the swelling kinetics and the absorbency of PANa-PAM in different swelling media? Is the swelling behavior of PANa-PAM more controlled by the chemical structures or the properties of the swelling media, such as the vacancy or the concentration of the ions in solution?

3) Will particle size of the PANa-PAM hydrogels affect the swelling behavior?

4) Will the properties of ionic solution also affect the mechanical properties of the swollen PANa-PAM hydrogels?

5) How will the PANa-PAM hydrogels react in mortar? What is the relationship between the effectiveness of PANa-PAM hydrogels on mitigating the autogenous shrinkage of mortar and the chemical properties of PANa-PAM?

CHAPTER 2. LITERATURE REVIEW

2.1 SAP Overview

2.1.1 Introduction

Superabsorbent polymers (SAPs) are three-dimensional hydrophilic crosslinked networks. Usually, the polymer chains contain ionized functional groups. When the hard, dry SAP particles are put into water or aqueous solution, they gradually turn into soft, rubbery hydrogels. These water-insoluble, hydrogel-forming polymers will absorb up to 1500g[14] of water per gram of polymer. Unlike traditional absorbent materials, such as soaked cotton or sponge, SAP particles can retain the absorbed fluid even under mechanical pressure. Figure 1 shows a dry and fully-swollen SAP particle.

The largest use of SAP particles is in hygiene industry, such as feminine sanitary napkins, infant diapers and adult diapers. Due to high water absorbency and ability to release water gradually, SAP particles also share a market in agricultural and horticulture industry. Other examples of SAP particles application are landscaping, food packaging, cable isolation, controlled release, water-absorbing construction materials.[15]

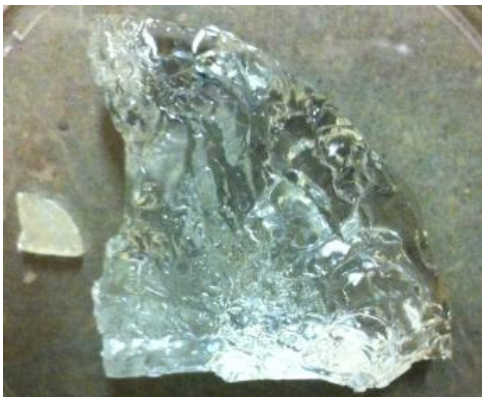

Figure 1. Synthesized poly(sodium acrylate-acrylamide) (PANa-PAM) with 67 wt.% PANa concentration and 2 wt.% crosslinking density in dry and swollen state (in deionized water for 2 days).

2.1.2 Synthesis of SAP

The primary commercialized superabsorbent polymer is crosslinked, partially neutralized poly(acrylic acid) due to its high charge-to-mass ratio.[16] Polyacrylamide is another commonly used material to make superabsorbent polymers because acrylamide can be easily polymerized to extra-high molecular weight (~10,000,000 g/mol)[17] which is preferable. Under high pH conditions, usually with a pH value of 12,[18] amide groups will hydrolyze to form anionic carboxylates. Until amide groups hydrolyze into carboxylic groups, polyacrylamide is a non-ionic polymer. Based on these two kinds of polymers, some other copolymers have also been studied as superabsorbent polymers, such as cassava starch-graft-polyacrylamide superabsorbents,[19] salt-resistant superabsorbent polymers made from poly(ethylene glycol), methacrylate, acryamide and partially neutralized acrylic acid,[20] and poly(acrylamide-co-sodium methacrylate) superabsorbent

polymers.[6] Besides these, some other superabsorbent polymers are also available such as cellulose-based superabsorbent polymers and alginate gels which are beyond the scope of this work.[16]

In general, there are two polymerization pathways to synthesize partially neutralized poly(acrylic acid) particles: solution polymerization[21] and suspension polymerization.[8] Crushed SAP particles made from solution polymerization have irregular shapes while SAP particles made from suspension polymerization are typically regular spheres.[22,23] According to Siriwatwechacul, *et al.*[11] solution polymerized SAP particles have increased water absorbency because suspension polymerization may form a denser, more tightly crosslinked hydrogel. In the present work, we chose solution polymerization to prepare SAP particles since regular shapes are not required for internal curing applications and we desire to obtain higher water absorbency of SAP particles for cement internal curing which will be discussed later.

Poly(acrylic acid) is often neutralized by sodium hydroxide to obtain partially neutralized poly(sodium acrylate) which is prepared by free radical polymerization from acrylic acid, sodium acrylate and crosslinker in aqueous system. The redox initiation system is often used to start the polymerization such as, ammonium persulfate and sodium

metabisulfite,[24] potassium persulfite and potassium metabisulfite,[25] sodium metabisulfite and sodium persulfate.[7] Neutralization of –COOH groups could be performed before the polymerization starts[7, 24] or after the crosslinked polymer network has formed.[26]

The covalent crosslinking molecules typically used in acrylic acid-based polymerization are di- and tri-acrylate esters such as ethylene glycol diacrylate.[27] N,N'-methylene-bis-acrylamide (MBA) is often used as a crosslinking agent for acrylamide polymerization. Raju, *et al.*[10] compared four crosslinking agents – MBA, ethylene glycol dimethacrylate (EGDMA), 1,4-butanediol diacrylate (BDA) and diallyl phthalate (DAP) – for preparation of poly(acrylamide-magnesium methacrylate-potassium acrylate). They found that SAP particles synthesized using MBA as the crosslinking agent had the greatest water absorbency over a range of crosslinking concentrations.

The post-polymerization procedure to remove residual monomers from poly(sodium acrylate) or polyacrylamide is to immerse the polymer gel in water for around 1-2 days.[6,7] This procedure is omitted in some published studies and instead the polymer gel is cut into pieces and dried in an oven directly after polymerization.[22] In the present

work, we assumed the polymerization to be fully completed and didn't take residue monomers into account.

2.1.3 Swelling Mechanism of SAP

The process of superabsorbent polymers absorbing water is to reach the equilibrium of the force resulting from elongation of polymer chain and the osmotic pressure which is caused by the difference of ion concentration inside and outside the polymers.[17]

When SAP particles are immersed in water, ionic groups along the polymer chain will form strong ion-dipole interaction with water molecules which facilitates water absorption. Due to electrical neutrality of the polymer, the charges from ionic groups spaced along the polymer chain must be matched by counterions (Figure 2). Large amount of counterions form the osmotic pressure which is the driving force for swelling. More ionic groups in the polymer chain will induce more counterions to the polymer network which leads to higher osmotic pressure. And higher osmotic pressure results in larger swelling absorbency.

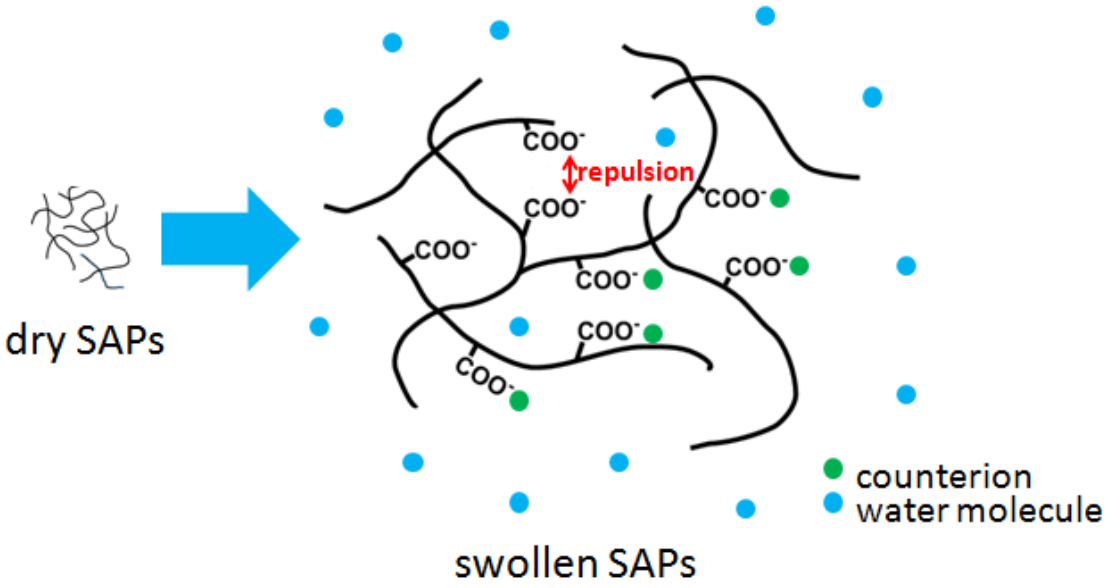

Figure 2. Schematic illustration of dry and swollen state of a poly(acylic acid) based SAP hydrogel particle.

As water molecules diffuse into polymer networks, polymer chains must move to accommodate the water and their favored random, coiled configuration is disturbed. The covalent crosslinks in the polymer system hinder the movement of polymer chains and prevent the polymer dissolve in water. It is obvious that a higher amount of covalent crosslinks inside the polymer network would lead to higher retraction force.

Eventually, the extensional force from the osmotic pressure balances the retraction force from the chemical or physical crosslinks inside the polymer network. As a result the polymer network reaches swelling equilibrium. Although the osmotic pressure is the driving force for swelling, we need to point out that the charged ionic groups along

polymer chains which tend to repel each other also contribute to the elongation force which pull polymer chains apart (Figure 2).

For non-ionic absorbent materials, the driving force for swelling is the formation of hydrogen bonds between polymer chains and water molecules and the increased entropy as decreased ordered structures during swelling. While for ionic superabsorbent polymers, high osmotic pressure and repulsion between polymer chains caused by ionic groups are the two most important contributors to the high absorbency. For this reason, we should be able to tune the absorbency of SAP particles by controlling the ratio of the ionic part to the non-ionic part. As we stated before, polyacrylamide is non-ionic polymer unless amide groups hydrolyze into $–COO^-$ groups at high pH. Since the ionic groups give rise to the osmotic pressure which drives the polymer network to swelling, it is plausible to tune the absorbency of polyacrylamide by controlling the hydrolysis degree. Also, it's reasonable to control the absorbency of partially neutralized poly(acrylic acid) by varying the neutralization degree of acrylic acid. Lastly it's manageable to incorporate acrylamide as a non-ionic monomer into poly(sodium acrylate) in order to control the swelling behavior of polymer network.

2.1.4 Factors that Influence the Absorbency of SAP

As stated before, the driving force of swelling for SAP is osmotic pressure which originates from the difference of the ion concentration inside and outside the polymer gel network. So the types of ions in swelling media which might act as the counterions in polymer network, ion concentration difference inside and outside the polymer network and also the chemical structures will affect the absorbency of SAP. Details will be discussed more in Section 2.2.

As for the real world cementitious application which will be discussed in Section 2.2, influence of particle size on absorbency of SAP particles should be taken into consideration. Large SAP particles may not be able to fully swell due to insufficient time for water uptake during the concrete mixing. So they could not supply every part of the cement during hydration which leads to a reduced efficiency. Small SAP particles are not preferable due to their less active surface zone compared to the bulk. [2]

Besides particle size, covalent crosslink density also plays an important role in determining the water absorbency of SAP particles. According to rubber elasticity theory,[28] the elastic shear modulus, *G*, of a crosslinked polymer network is related to

the molecular weight of the polymer chain between neighboring crosslinks. The equation to describe this is as follows:

$$G \approx \frac{nkT}{V} \approx \frac{\rho RT}{Ms} \qquad \text{Eq. 1}$$

where n / V is the number of elastically active network strands per unit volume, k is the Boltzmann constant, T is the temperature, R is the gas constant, ρ is the mass per unit volume (*i.e.*, the network density), and M_S is the average molecular weight of between two crosslink points. Thus, the elastic shear modulus of a crosslinked hydrogel will increase as the concentration of crosslinks in the network increases.[29] During the swelling process for PANa-PAM hydrogels, an equilibrium is reached between elongation force which comes from osmotic pressure and the retraction force which originates from the network's elastic shear modulus.[17] Thus, as covalent crosslinking density increased in the PANa-PAM hydrogel samples, the elastic shear modulus increased which led to larger retraction forces within the network and a corresponding decrease in swelling ratio.

The effect of pH value of swelling media may also affect the absorbency of SAP but this effect depends on the chemical structure of SAP since only ionic groups along the

polymer chain give rise to osmotic pressure. One could imagine that if the polymer chain only contains –COONa groups instead of pH-sensitive ionic group, such as –COOH, pH value of the swelling media may not affect the absorbency of SAP at all, which is also been found in our research. For partially neutralized poly(acrylic acid) SAP or other pH sensitive hydrogels, pH value of the swelling media is also a major concern when evaluate the absorbency of SAP. For example, Yarimkaya[8] synthesized a pH-sensitive acrylate-based hydrogel. He found that when the pH of the swelling medium increased from 3.0 to 5.0, which is above the pKa value of acrylic acid, the final swelling value of this hydrogel increased sharply. As pH goes up, carboxyl groups along the polymer chains will deprotonate which leads to negatively charged polymer chains. Large amount counterions come into the hydrogel which results in a high osmotic pressure and the negatively charged polymer chains repel each other. Thus the deprotonated poly(acrylic acid) can absorb much more water than pure poly(acylic acid).

The influence of neutralization degree of acrylic acid on swelling ratio of SAP particles is similar to that of pH value. Chen[7] investigated how the neutralization degree of poly(acrylic acid-co-acrylamide) affects water absorption of the gel. It is reported that as neutralization increased to 75%, the water absorbency of SAP particles went up which could be explained by increased osmotic pressure. But the water absorbency decreased

after further increased neutralization degree. They believed over-neutralization has negative effects on the dissociation of sodium acrylate and that would freeze the polymer chain segment.

The temperature of the swelling media is another factor which affects the absorbency of SAP particles that most researchers looked into. However, temperature seems not a major influence on the absorbency of SAP particles. The absorbency of acrylic acid based SAP particles only showed small fluctuations within 0-100°C range.[9,7]

2.2 Application of SAP in Concrete

2.2.1 Internal Curing for High Performance Concrete (HPC)

High Performance Concrete (HPC) has increased strength and denser microstructures than ordinary concrete due to lower water/cement (w/c) and the addition of silica fume.[30] However, the major limitation of HPC is the occurrence of autogenous shrinkage in the early stages of curing which can lead to cracking and compromised strength.[31] As the hydration process proceeds and water is consumed, vapor filled pores begin to form as the system self-desiccates. The decreasing air-water menisci lead to lower internal relative humidity (RH) and larger capillary tension in the pore fluid which results in

compressive bulk stress on cement paste. Autogenous shrinkage happens in this circumstance. [1,32]

Internal curing is considered to be an effective method to reduce self-desiccation. By incorporation of materials with high water storage capacity, referred to as internal curing agents, the stored water can be released into the concrete matrix during the curing process in order to mitigate self-desiccation.[33] Internal curing has been examined by researchers for more than 20 years[34,35] and has recently begun to be implemented on bridges in New York,[36,37] Indiana,[38,39] and Utah.[40]

Lightweight aggregate (LWA) is one class of internal curing agents and has been found to be very effective at reducing or eliminating autogenous shrinkage.[41,42] Yet incorporation of LWA would compromise the final compressive strength of concrete through the formation of voids and flaws in the cured concrete that display a range of sizes and morphology.[43]

2.2.2 SAP Particles as Internal Curing Agent

Another widely studied class of internal curing agents is superabsorbent polymers (SAPs). The most common SAP hydrogels used for internal curing are composed of

covalently crosslinked poly(acrylic acid-acrylamide) molecules.[16] The carboxylic acid groups of the acrylic acid monomer will deprotonate at pH > 5 (forming an anionic moiety, whereas the amide groups of the acrylamide monomer are partially hydrolyzed to form anionic carboxylic groups along the polymer chain when pH is ~12 or above.[11,18] Other times, partially neutralized acrylic acid (*e.g.*, sodium acrylate) is directly used for synthesis, which, when exposed to water, will readily form anionic groups.[7]

When SAP is added to concrete mixtures, SAP particles provide a continuous supply of water during curing, thus reducing/eliminating autogenous shrinkage and cracking of the concrete and achieving a corresponding increase in concrete durability.[1,44,45] Although, dehydrated SAP particles will leave voids which may compromise the final strength but the shape of voids, pore size distribution and the absorption capacity of internal curing agent can be controlled by designing SAP particles.[1] Furthermore, addition of SAP particles in concrete changes the dynamics of concrete hydration process. Justs, *et al.*[46] found that addition of small amount of SAP into cement paste (w/c=0.2) would make the hydration process of cement paste start earlier and proceed at a slower rate. Hydration degree measured at 3 days showed that the entrained water by SAP increased the hydration degree in a same manner as increase w/c. The same result showing that SAP would help increase the hydration degree of cement paste was

reported by Esteves.[47] As a result, incorporated SAP particles into concrete may increase the final compressive strength by increasing hydration degree of concrete.

Though many of the benefits of incorporating SAP particles into concrete have been defined in the past, research is still uncovering additional benefits, such as the ability of SAP particles to enhance the freeze/thaw resistance of concrete,[48–50] to reduce thermal expansion,[51] or to heal cracks.[52]

2.2.3 SAP Swelling in Cement Pore Solution

SAP particles are polymer hydrogels composed of polyelectrolyte (charged polymer) chains which are covalently crosslinked to form a three-dimensional polymer network. Driven by osmotic pressure, dry SAP particles swell when in contact with an aqueous fluid (see Figure 2).[17] Osmotic pressure results from the formation of a chemical potential gradient in the system due to the relatively high concentration of ions within the SAP's polymer network compared to the external environment.

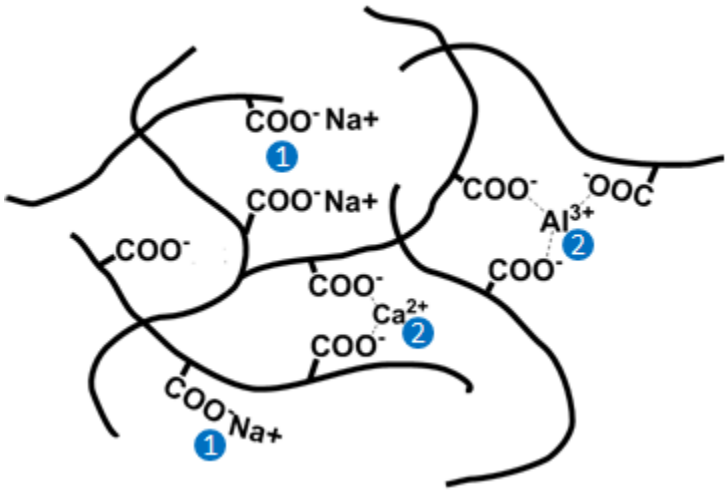

Figure 3. Schematic illustrating the state of a poly(acrylic acid) based SAP hydrogel particle swelling in cement pore solution. Label (1) indicates the screening effect by Na^+ which reduces the repulsion force between carboxylic groups. Label (2) indicates potential ionic crosslink formation with multi-valent ions in the fluid which hinders swelling.

During the hydration process of concrete, multiple ions such as K^+, Na^+, OH^-, and Ca^{2+} are released into the pore solution.[53] In general, the diffusion of ions into a SAP particle leads to deswelling of the hydrogel because the ions effectively screen the repulsive interactions between charged groups within the polymer network. This screening reduces the driving force of swelling and is illustrated in Figure 3 with Na^+ ions and anionic carboxylic groups in a poly(acrylic acid) polymer network. Calcium ions, Ca^{2+}, have been found to have a particularly strong effect on the overall absorbency and swelling kinetics of SAP particles.[7,11,18] Jar, *et al.*[18] found that divalent cations have stronger interactions with polyacrylamide-based gels than monovalent cations. Recently, Schröfl, *et al.*[3] showed that the presence of Ca^{2+} in the aqueous fluid will dramatically

decrease the absorption capacity and alter the absorption and release kinetics of commercial SAP particles. This ionic interaction ultimately resulted in increased autogenous shrinkage and decreased compressive strength of the final cured concrete product. In addition to Ca^{2+}, magnesium ions (Mg^{2+}) have similar effects on the swelling behavior of SAP particles.[9]

CHAPTER 3. EXPERIMENTAL METHOD

3.1 Materials

Acrylic acid (AA), acrylamide (AM), N,N'-methylenebisacrylamide crosslinking agent (MBA), sodium metabisulfite ($Na_2S_2O_5$), sodium persulfate ($Na_2S_2O_8$), sodium hydroxide (NaOH), sodium chloride (NaCl), calcium nitrate tetrahydrate ($Ca(NO_3)_2 \cdot 4H_2O$), aluminum sulfate hydrate ($Al_2(SO_4)_3 \cdot H_2O$), calcium sulfate ($CaSO_4$), potassium hydroxide (KOH), potassium sulfate (K_2SO_4), aluminum sulfate ($Al_2(SO_4)_3$), ethylenediaminetetraacetic acid disodium salt concentrate (for 1 L standard solution, 0.1 M EDTA-Na_2), Eriochrome® Black T, magnesium chloride ($MgCl_2$), ammonia buffer solution (pH = 10), methanol were purchased from Sigma-Aldrich and were used as received. Deionized water used in the experiment was produced from a Nanopure® Infinity Barnstead water purification system. Portland cement type I (Greencastle Plant) was used to obtain pore solution for swelling study. The chemical composition of this cement is shown in Table 1.

Table 1. Chemical composition of Portland cement Type I (mass%)

SiO_2	Al_2O_3	Fe_2O_3	CaO	MgO	SO_3	Total alkali(Na_2O+0.658K_2O)	Insoluble Residue
19.6	5.2	2.9	64.0	2.6	3.3	0.72	0.21

3.2 PANa-PAM Hydrogel Preparation

Poly(sodium acrylate-acrylamide) (PANa-PAM) was synthesized through free radical solution polymerization of 100 wt.% neutralized acrylic acid and acrylamide monomer according to Horkay*, et al*.(see Figure 4).[26,54] As acrylic acid is neutralized before polymerization, this will result in a polymer network in which the anionic groups are from the acrylic acid segments of the chain (*i.e.*, COO^-) and the acrylamide segments remain intact and subsequently un-charged. NaOH solution was used to neutralize the acrylic acid monomer prior to synthesis. Redox initiator solution was obtained by separately dissolving $Na_2S_2O_5$ and $Na_2S_2O_8$ in deionized water to concentrations of 0.5 wt.%. Aqueous solutions of MBA were used for crosslinking. These solutions were prepared 1 day in advance to allow MBA powder to dissolve fully. The covalent crosslinking densities used in present work were 1.0 wt.%, 1.5 wt.% and 2.0 wt.% (by monomer weight) and initiator concentration was 1 wt.%. For each selected covalent crosslinking density, the ratio of acrylic acid to acrylamide was varied as: 0 wt.% PANa, 17 wt.% PANa, 33 wt.% PANa, 67 wt.% PANa, 83 wt.% PANa.

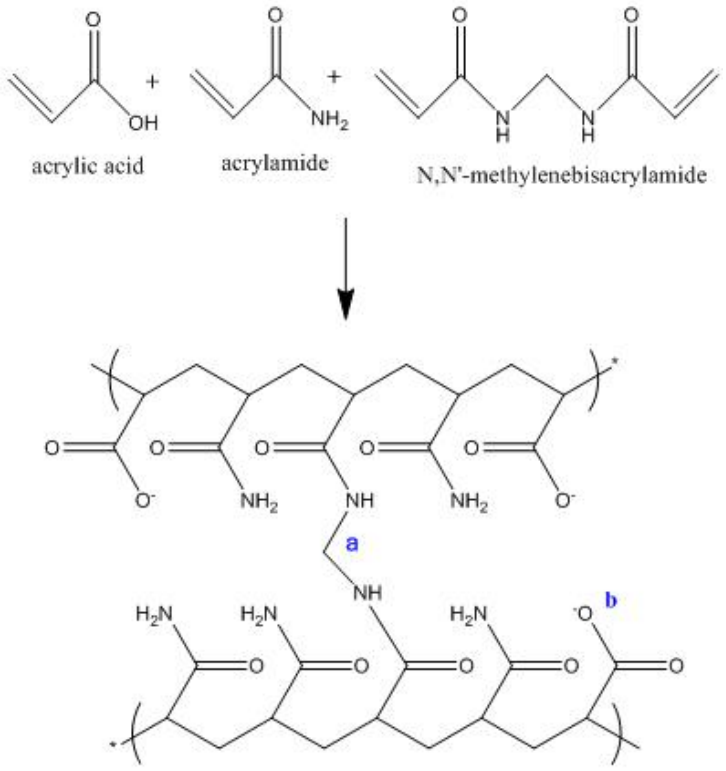

Figure 4. Reaction scheme of PANa-PAM hydrogel. The polymer network of the hydrogel contains covalent crosslinks (a) and anionic carboxylate groups (b).

To perform the synthesis, the initiator solution was added to a mixture of neutralized acrylic acid, acrylamide, and crosslinking agent and stirred. An exothermic reaction began within a few seconds for the pure acrylamide system (*i.e.*, 0 wt.% PANa). The reaction occurred rapidly (few minutes) and a clear hydrogel was observed to form. For other PANa-PAM ratios, the formation time varied from a few minutes to few hours. All vials were allowed to rest for another 24 hours, at least, after the gel formation to ensure reaction completion. To obtain the hydrogel, the glass vial was crushed. All the hydrogel samples were elastic and thus retained the cylindrical shape of the vial.

Hydrogel samples were washed with water and crushed to form smaller pieces, which were then dried overnight at 80℃. Dried PANa-PAM particles were then ground further into fine particles (using a mortar and pestle). Using a series of sieves, two final (dry) particle size distributions were obtained: 106-425 μm and 425-850 μm. Another set of hydrogels were cut into quarters followed by drying overnight at 80℃ for macroscale swelling studies and mechanical testing.

For autogenous strain or internal humidity of tests performed on mortar samples, only PANa-PAM hydrogels with 17 wt.% PANa (SAPI) and 67 wt.% PANa (SAPII), 2% crosslinking agent, were picked. The samples were synthesized as discussed before but instead of using mortar and pestle to grind the sample, ball milling technique was used to obtain fine particles. The dried polymer pieces were put in a plastic bottle with ceramic milling media and the bottle was left rolling overnight with a speed 50r/h to get particles size within 45-106μm.

3.3 Swelling Study

The gravimetric "teabag" method was used to evaluate the overall swelling capacity and kinetics of the PANa-PAM hydrogel samples.[7,20] Four different immersion solutions were studied: pure deionized water, 0.025 M Na^{+} (from NaCl), 0.025 M Ca^{2+} (from $Ca(NO_3)_2 \cdot 4H_2O$), and 0.025 M Al^{3+} (from $Al_2(SO_4)_3 \cdot H_2O$).

The measurement procedure was as follows: 0.2 g dry sample were added into a pre-wetted teabag and immersed in 200 ml of solution. For 425-850 µm samples, the wet mass was measured after immersion times of 1, 3, 5, 10, 15, 30, 60, 120, and 240 minutes; for 106-425µm samples, the wet mass was measured after immersion times of 30s, 1, 2, 5, 10, 15, 30, 60, and 120 minutes. The mass was measured after absorbing excess water from the teabag's surface using a paper towel. In this project, macroscale PANa-PAM samples (0.35-0.45 g dry, ~8 mm × 8 mm × 5 mm in dimension) were also studied for comparison purposes. For the macroscale samples, teabags were not used to assist in the swelling measurement. Immersion volumes of 500 ml were used for these larger samples and the wet mass was tracked for 10 days. For all PANa-PAM samples, the swelling ratio, *Q* (g/g), was calculated from the following equation:

$$Q = \frac{m_s - m_d}{m_d} \qquad \text{Eq. 2}$$

where m_s was the wet mass of the swollen samples and m_d was the initial dry mass. Samples used for swelling measurements were from different synthesis batches, and measurements were repeated 3 times.

The absorbency of PANa-PAM particles (106-425 µm, 2 wt.% covalent crosslinking density) in synthetic pore solution was also studied. 0.2g of dry sample was immersed in

50ml pore solution. The swelling study was performed in synthetic pore solution instead of extracted pore solution from concrete due to enormous time consuming to get extracted pore solution. The composition of synthetic pore solution is based on previous literature[55] with addition of small amount of aluminum sulfate. The composition of synthetic pore solution is reported in Table 2. The synthetic pore solution was prepared and stored in a plastic bottle with cap.

Table 2. Chemical composition of synthetic pore solution (mM)

Na^+	K^+	Ca^{2+}	OH^-	SO_4^{2-}	Al^{3+}
117	684	2	632	86	3.2

3.4 Quantify Ca^{2+} by Titration

The Ca^{2+} that remained in the immersion solution after the sample reached swelling equilibrium was quantified by basic titration methods.[56] Calcium ion solutions were titrated by EDTA solution, and Eriochrome® Black T was used as the indicator. To prepare the indicator solution, 0.1g Eriochrome Black T is added to 20g methanol and fully mixed. The indicator solution is prepared fresh every few days and kept in a vial covered with tin foil. The 0.01M ETDA standard solution was obtained by diluting the EDTA-Na_2 solution to a 10L.

To perform the titration, the 0.01M EDTA standard solution was poured into a 100ml buret and 25ml calcium solution was transferred into a narrow-mouth flask. 0.5ml Mg-EDTA solution (mixing same volume of 0.01M EDTA standard solution and 4M $MgCl_2$ aqueous solution) was added to the test solution for a sharper color change. Also 2ml ammonia buffer solution and 5-6 drops of indicator solution was added to the test solution. Add roughly 50ml distilled water and shake the flask to mix chemicals. During the titration, pay attention to the color of the solution. Around the end point, add the EDTA solution drop by drop, shake the flask fully and wash the inner wall of flask by distilled water until the color turns to pure blue.

3.5 DMA and MTS Tests

PANa-PAM hydrogel samples that were swollen in Ca^{2+} solutions were tested in compression by dynamic mechanical analysis (DMAQ800, TA Instruments) to obtain the stress response as a function of strain for each sample. The mode was “force control”, preload force was 0.1 N, and the force ramp was 0.2 N/min. The samples were cut into 6-mm×6-mm×4-mm cubes for compression testing.

PANa-PAM hydrogel samples swollen in Al^{3+} solutions did not display isotropic properties (as described in the results section) and could not be cut into the smaller samples that were required for testing with the DMA. Therefore, these samples were

tested under compression mode with an MTS mechanical testing load frame with compression platens. Samples were roughly 1/4 of a round disc with diameter of 20mm and thickness of 10mm The preload force was 1 N and load rate was 1 mm/min. Data was collected regardless of the unusual sample shape in order to have an overall evaluation of the sample's mechanical properties. In the future, more regular disc shapes will be synthesized. Rectangular strips (5-mm×3-mm×0.5-mm) of the stiff outer region of the PANa-PAM hydrogel samples swollen in Al^{3+} solutions were tested in tension with the DMA.

3.6 Mortar Composition, Mixing and Testing

In order to evaluate the efficiency of PANa-PAM to decrease the autogenous shrinkage of mortar, we prepared plain mortar sample and modified mortar samples by SAP. The composition of mortar tested in this work is reported in Table 3. Mortar composition and the w/c is 0.3. The extra added water for PANa-PAM to absorb is 0.05 by weight of cement. The amount of SAP needed in the mortar sample was calculated based on the absorbency of PANa-PAM hydrogels in pore solution which was obtained by mixing Portland cement type I with water.

Table 3. Mortar composition

Materials	Cement	Free Water	Internal Curing Water	Fine aggregates	SAP
Amount (kg/m^3)	666	200	35.5	1440	0 (plain) 3.09 (SAPI) 2.22(SAPII)

The mixing procedure was followed by ASTM C305 with only minor modifications.[57] Based on our past experience, small amount of water reducer was added into the mortar to maintain workability while avoiding segregation and excessive bleed water; 3.5 ml/kg, 5.5 ml/kg and 1.0 ml/kg of water reducer (by weight of cement) was used for the plain mixture, mixture with SAPI and mixture with SAPII, respectively. The amount of water reducer added into the mixture is dependent on the workability of the mortar mixture. The mortar mixture with SAPII initially had good workability even though only 0.8g of water reducer was added during mixing; however, much of this workability was lost as samples were cast. Because specimens were successfully made, even with the decreased workability, no further action was taken to readjust the workability.

In order to evaluate the efficiency of PANa-PAM hydrogels on mitigating the autogenous shrinkage of cementitious material, the autogenous strain was monitored in the mortar samples. ASTM C1698-09[58] was followed to measure the autogenous strain of mortar

samples using a dilatometer with corrugated tubes. The mortar mixture was cast into corrugated tubes under vibration and for each mortar mixture, two corrugated tubes were filled and carefully sealed by tape (see Figure 5). The tubes were double checked to verify no air bubbles were present and were placed in a room with constant temperature (23 °C). The autogenous strain of mortar mixtures was monitored for 9 days after mixing using LVDTs.

Also internal relative humidity (RH) data of plain mortar samples and mixtures with SAP particles were collected. The same mortar mixtures as used for autogenous shrinkage were placed in airtight containers and set for 48 h before internal humidity test. The HC2-SH sensor (±0.5 %RH at 23 °C ±5 K) for measuring the humidity is offered by Rotronic company. Relative humidity probes were calibrated before each test with saturated salt solutions and were mounted in a 75 mm × 68mm stainless steel cylinder that was placed over a water jacketed sample cup holder (see Figure 6). The water jacket was connected to a water bath at a constant temperature of 25°C. The mortar samples were crushed and sealed inside of the chamber, where the RH was then monitored for 7 days.

Figure 5. Sealed corrugated tubes filled with mortar mixture for autogenous strain test.

Figure 6. Rotronic chambers for relative humidity tests.

CHAPTER 4. RESULTS AND DISCUSSION

4.1 Swelling Study of Microscale Samples

4.1.1 Swelling Study in Water and Na^+ Solutions

Figure 7 and Figure 8 displays the transient swelling ratio for PANa-PAM hydrogel samples containing different concentrations of PANa in deionized water and Na^+ solutions. After a quick initial intake of water at short times, the swelling ratio reached an effective plateau within approximately 50 minutes for all the hydrogel samples. In general, the maximum swelling ratio and the initial swelling rate were observed to increase for hydrogels that contained greater concentrations of PANa in the polymer network. For example, for a hydrogel sample with 2 wt.% covalent crosslinking density, the initial swelling rate in Na^+ solution was 3.7 $(g/g)min^{-1}$ for the 17 wt.% PANa sample and increased to 9.0 $(g/g)min^{-1}$ for the 83 wt.% PANa sample (note: both rates were calculated for the first 5 min of immersion).

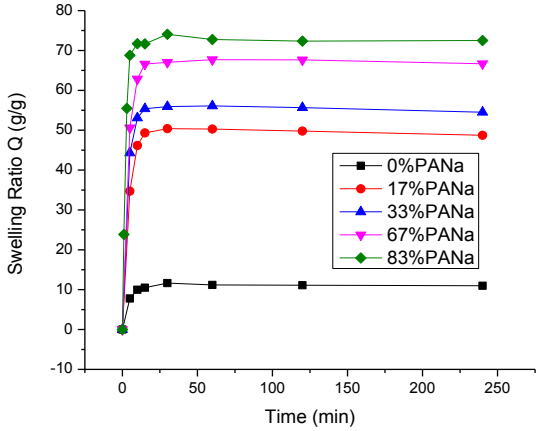

Figure 7. Absorption of 425-850µm PANa-PAM hydrogel samples with 2 wt.% covalent crosslinking density in deionized water.

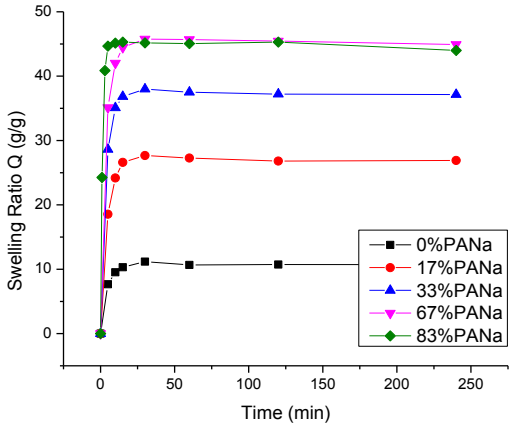

Figure 8. Absorption of 425-850µm PANa-PAM hydrogel samples with 2 wt.% covalent crosslinking density in Na^+ solution.

Table 4. Equilibrium (long-time) swelling ratios, *Q* (g/g), of 425-850 µm PANa-PAM hydrogel samples immersed in pure deionized water, 0.025 M Na^+, 0.025 M Ca^{2+}, and 0.025 M Al^{3+} solutions.

		PANa Concentration (in polymer network)				
Covalent Cross-linking	Solution	0 wt.%	17 wt.%	33 wt.%	67 wt.%	83 wt.%
1.0 wt.%	H_2O	14.9	105.1 ± 7.9	89 ± 24.9	116.1 ± 5.9	125.0 ± 3.9
	Na^+	14.3	43.3 ± 3.0	47.5 ± 11.1	60.5 ± 3.1	62.7 ± 6.1
	Ca^{2+}	14.1	11.1 ± 2.7	10.6 ± 5.1	2.9 ± 0.4	1.9 ± 0.3
	Al^{3+}	13.4	3.4 ± 0.1	2.6 ± 0.3	8.6 ± 3.2	13.3 ± 7.0
1.5 wt.%	H_2O	13.9	65 ± 12.5	67.6 ± 26.5	90 ± 15.4	113.4 ± 20.6
	Na^+	13.2	32.5 ± 3.1	41.6 ± 14.4	53.3 ± 6.5	59.8 ± 6.8
	Ca^{2+}	11.4	11.7 ± 1.8	6.8 ± 0.2	3.0 ± 1.5	1.9 ± 0.5
	Al^{3+}	11.5	2.8 ± 0.8	2.4 ± 0.4	5.3 ± 1.0	7.1 ± 2.3
2.0 wt.%	H_2O	11.0	41.7 ± 13.8	50 ± 7.9	68.2 ± 6.5	74.3 ± 8.3
	Na^+	10.7	23.3 ± 4.7	33.2 ± 4.6	41.3 ± 4.2	44.8 ± 3.2
	Ca^{2+}	10.8	8.2 ± 1.4	7.1 ± 0.4	2.7 ± 0.5	2.2 ± 0.1
	Al^{3+}	9.4	2.9 ± 1.0	2.6 ± 0.7	3.3 ± 2.2	8.7 ± 5.4

The final swelling ratio at long times (*e.g.*, ~ 4h) was known as the equilibrium swelling ratio and is reported in Table 4 for PANa-PAM hydrogel samples containing different covalent crosslinking densities and PANa concentrations. For all the samples, the equilibrium swelling ratio obtained from immersion in Na^+ solutions was reduced compared to the swelling ratio in deionized water. Consistent with Figure 7 and Figure 8,

PANa-PAM hydrogel samples that contained greater concentrations of PANa in its polymer network displayed a correspondingly increased equilibrium swelling ratio from immersion in water and Na^+ except for one abnormal point (H_2O, 33 wt% PANa, 1% crosslinking density). This odd point might result from imperfection of synthesis. More controlled synthesis methods will be investigated in the future.

Table 4 also indicates that increased covalent crosslinking density led to decreased swelling ratio for samples immersed in deionized water or Na^+ solutions. For 17 wt.% PANa sample, the swelling ratio decreased from 105.1 g/g to 41.7 g/g (in water) and from 43.3 g/g to 23.3 g/g (in Na^+ solution) as the covalent crosslinking density increased from 1 wt.% to 2 wt.%. This trend is consistent with published results; for example, the swelling ratio of poly(acrylamide-co-sodium methacrylate) decreased from 250g/g to140g/g as the concentration of crosslinking agent (MBA) increased from 0.016 mM to 0.032 mM.[6]

The swelling behavior of hydrogel samples in solutions containing different ion concentrations was also investigated (Figure 9). As shown in Figure 9a, the equilibrium swelling ratio of a representative hydrogel sample decreased as the Na^+ ion concentration of the swelling solution increased from 0.0125 M to 0.1 M. The swelling rate also decreased as ion concentration increased (shown in Figure 9b). For example,

the hydrogel sample immersed in 0.0125 M solution increased to 61 g/g within the first 5 minutes while the sample immersed in 0.1 M solution only reached 30 g/g.

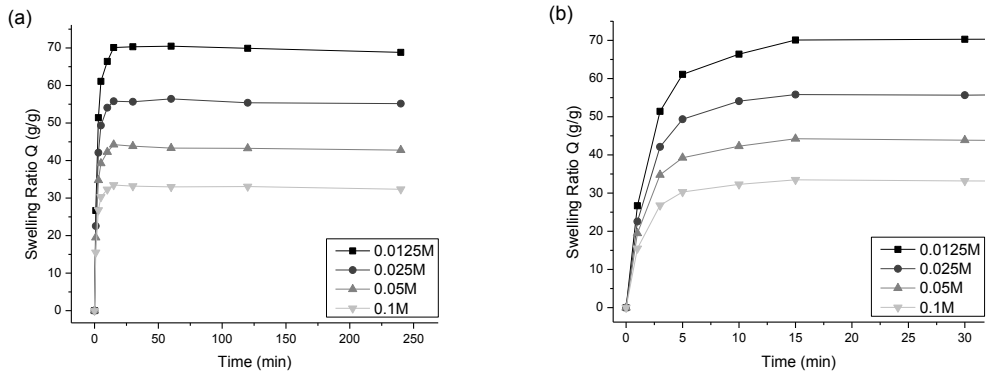

Figure 9. Swelling behavior of 425-850µm 33 wt.% PANa, 1 wt.% covalently crosslinked PANa-PAM hydrogel sample immersed in Na^+ solutions with varying ion concentrations over the full immersion time of 240 min (a) and during the first 30 min of immersion (b).

Discussion

The driving force for swelling (*i.e.*, osmotic pressure) was related to the ion concentration difference internal and external to the hydrogel sample, referred to here as the ion concentration gradient. In the PANa-PAM hydrogels that were studied, the concentration of anionic groups within the hydrogel was directly proportional to the amount of PANa within the polymer network, which varied according to the selected monomer feedstock ratio used for the hydrogel synthesis. Thus, the PANa-PAM hydrogel samples with higher PANa concentrations had greater internal ion concentrations which explains the increased swelling ratios reported in Table 4 when

immersed in the same swelling media (deionized water or 0.025 M Na^+). Likewise, the swelling ratio of a given PANa-PAM hydrogel sample directly depends upon the ion concentration of the immersion solution. From Table 4, the equilibrium swelling ratio was higher for all the PANa-PAM hydrogel samples immersed in deionized water (larger ion concentration gradient) than in Na^+ solutions (smaller ion concentration gradient). The relationship was further confirmed by immersing samples in Na^+ solutions with different ion concentrations (Figure 8). Swelling was reduced for PANa-PAM hydrogels immersed in solutions containing higher concentrations of Na^+.

As stated in Section 2.1.4, the crosslinking density of the polymer network affects the swelling ratio of SAP particles. As covalent crosslinking density increased in the polymer network, the elastic modulus increased which gives rise to larger retraction force with the polymer network. So the equilibrium swelling ratio decreased as crosslinking density increased in PANa-PAM hydrogel samples (see Table 4). Experiments were performed to measure the mechanical properties of the hydrogel samples and these are described in Section 4.2.2.

4.1.2 Swelling Study in Ca^{2+} and Al^{3+} Solutions

Figure 10 and Figure 11 displays the swelling behavior for hydrogel samples with different PANa concentrations immersed in Ca^{2+} and Al^{3+} solutions. In Ca^{2+} solutions, the

equilibrium swelling ratios decreased as PANa concentrations increased (Figure 10, average values reported in Table 4). For example, for a hydrogel sample in Table 4 with 2 wt.% covalent crosslinking density immersed in Ca^{2+} solutions, the swelling ratio decreased from 8.2 g/g to 2.2 g/g as the PANa concentration increased from 17 wt.% to 83 wt.%. In Al^{3+} solutions, the equilibrium swelling ratios decreased and then increased as PANa concentrations increased (Figure 11, average values reported in Table 4). For 17 wt.% and 33 wt.% PANa concentration samples, the swelling ratio in Ca^{2+} solutions was larger than in Al^{3+} solutions while for 67 wt.% and 83 wt.% PANa concentration samples, the swelling ratio in Ca^{2+} solutions was smaller than in Al^{3+} solutions.

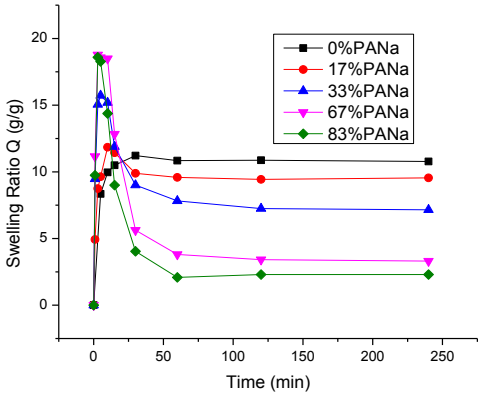

Figure 10. Absorption of 425-850μm PANa-PAM hydrogels with 2 wt.% covalent crosslinking density in Ca^{2+} solution.

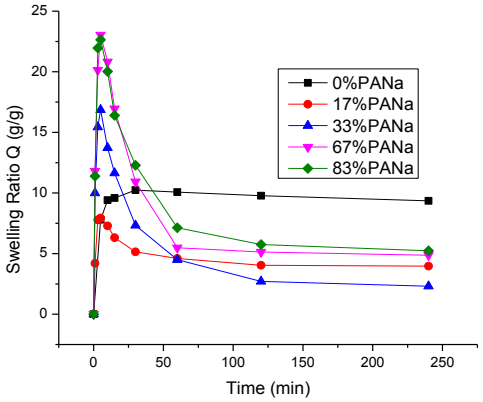

Figure 11. Absorption of 425-850µm PANa-PAM hydrogels with 2 wt.% covalent crosslinking density in Al^{3+} solution.

As shown in Table 4, the equilibrium swelling ratios of hydrogels immersed in Ca^{2+} and Al^{3+} solutions were significantly reduced compared to the ratios of samples swollen in water and Na^{+}. For example, the swelling ratio of a 33 wt.% PANa, 2 wt% crosslinking density sample decreased from 33.2 g/g in Na^{+} solution to 7.1 g/g in Ca^{2+} solution and 2.6 g/g in Al^{3+} solution. Compared with the swelling behavior of samples immersed in deionized water or Na^{+} solutions, the covalent crosslinking density did not have a significant effect on the samples immersed in Ca^{2+} or Al^{3+} solutions (see Table 4). For example, the swelling ratio for 67 wt.% PANa concentration samples was around 3.0 g/g (immersed in Ca^{2+} solutions) for 1 wt.%, 1.5 wt.%, or 2 wt.% covalent crosslinking density. Additionally, the samples immersed in Al^{3+} solutions appeared to become much stiffer (mechanically) compared with other samples.

The swelling kinetics were also observed to change when hydrogel samples were immersed in Ca^{2+} and Al^{3+} solutions compared with the behavior observed during immersion in pure water or Na^{+} solutions. At short immersion times, an obvious peak was observed for samples containing PANa in the polymer network while no significant peak was observed for the 0 wt.% PANa sample (*i.e.*, 100 wt.% PAM). The peaks in the swelling responses indicated a rapid swelling of the hydrogel sample immediately followed by a de-swelling or release of fluid from the sample. In both Figure 10 and Figure 11, hydrogel samples containing a majority concentration of PANa attained the greatest short-time swelling ratios (*i.e.*, displayed the highest peaks). Additionally, the peaks for samples immersed in Ca^{2+} solution became narrower as PANa concentration increased (Figure 10) while the peaks became broader as PANa concentration increased for samples immersed in Al^{3+} solution (Figure 11). Similar to results in Section 4.1.4, the initial swelling rate increased as PANa concentration increased but the trend was much weaker. For example, for a hydrogel sample with 2 wt.% covalent crosslinking density, the initial swelling rate in Ca^{2+} solution was 1.9 $(g/g)min^{-1}$ for the 17 wt.% PANa sample and increased to 3.7 $(g/g)min^{-1}$ for the 83 wt.% PANa sample (note: both rates were calculated for the first 5 min of immersion).

To determine the amount of Ca^{2+} ions absorbed by the hydrogel samples, titration was performed on the immersion solution remaining after a hydrogel sample was allowed to

swell and reach equilibrium in Ca^{2+} solution for 4 h. The amount of Ca^{2+} absorbed by each sample was calculated by subtracting the amount of Ca^{2+} consumed by titration from the initial Ca^{2+} added in the swelling media (*i.e.*, 0.025M). Figure 12 shows the concentration of absorbed Ca^{2+} ions as a function of PANa concentration in the polymer network of the hydrogel sample. Greater concentrations of Ca^{2+} ions were absorbed by polymer networks containing greater PANa concentrations.

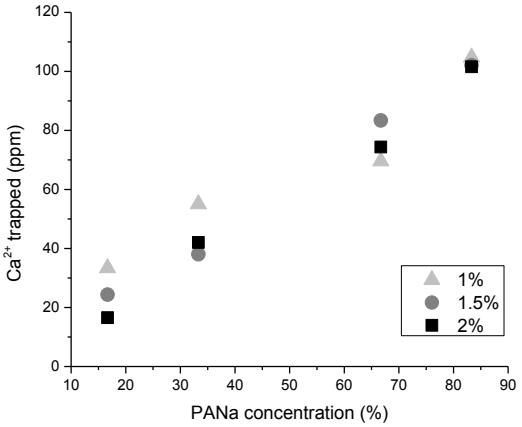

Figure 12. The concentration of Ca^{2+} trapped by 425-850µm PANa-PAM hydrogels with 1 wt.%, 1.5 wt.%, 2 wt.% crosslinking density after 4 h immersion time (as determined by titration).

Discussion

As observed in Figure 9 and Figure 10, the overall absorption capacity and swelling kinetics of PANA-PAM hydrogel samples immersed in multi-valent Ca^{2+} or Al^{3+} solutions were dramatically different compared with hydrogel samples swollen in pure water or

Na^+ solutions. The equilibrium swelling ratio decreased for hydrogels immersed in the multi-valent solutions, and the reduction was strongest for hydrogels containing greater concentrations of PANa in the polymer network. Swelling kinetics of the hydrogels immersed in the multi-valent solutions displayed fast swelling immediately followed by fast fluid release. Additionally, post-swelling titration analysis displayed in Figure 12 indicated that the largest concentrations of Ca^{2+} ions were trapped by the hydrogel samples containing the greatest concentrations of PANa.

The reduced PANa-PAM hydrogel swelling in Ca^{2+} and Al^{3+} solutions compared with those swollen in water or Na^+ solutions is believed to be due to the diffusion of Ca^{2+} or Al^{3+} ions into the hydrogel network and the subsequent formation of complexes or "ionic crosslinks" with the anionic groups in the polymer network (derived from incorporation of PANa into the network). This explanation is consistent with the results shown in Figure 10, Figure 11 and Figure 12, illustrating that PANa-PAM hydrogel samples which contained a greater concentration of PANa were more sensitive to the presence of multi-valent ions, displaying greater reductions in swelling and a greater absorption of Ca^{2+}. It is inferred that polymer networks within the PANa-PAM hydrogel samples were more sensitive to trivalent ions (Al^{3+}) than divalent ions (Ca^{2+}) due to the fact that the samples containing 17 and 33 wt.% PANa have a more reduced equilibrium swelling ratio in Al^{3+} solutions than in Ca^{2+} solutions (note: the reverse is true for

samples contianing >33 wt.% PANa and this is explained in Section 4.2). Additionally, ionic crosslinking propensity had a much stronger impact on swelling behavior than the concentration of covalent crosslinks even for samples with small amounts of PANa.

Additionally, the observed change in swelling kinetics due to the presence of multi-valent ions was most likely related to the time-dependent formation of ionic crosslinks within the polymer network of the hydrogel. At short immersion times, PANa-PAM hydrogel samples containing relatively high concentrations of PANa displayed greater overall absorption and faster swelling rates due to the correspondingly large ion concentration gradient driving the swelling response. However, as the ions diffuse over time and form ionic crosslinks, samples containing a greater concentration of PANa formed a proportionally greater concentration of ionic crosslinks within the polymer network, leading to a large reduction in swelling and the formation of the swelling peaks in Figure 10 and Figure 11. This internal competition between swelling due to ion concentration gradients and deswelling from ionic crosslinking explains why in Figure 10 and Figure 11 the maximum value of the short-term swelling ratio peak approaches a limiting value even though the concentration of PANa in the polymer network continued to increase (*e.g.*, from 67 wt.% to 83 wt.%).

The overall reduction of swelling due to the presence of ionic crosslinks between multi-valent ions and the polymer network of the hydrogel samples is most likely due to a combination of (1) physical restriction of the polymer chains (*i.e.*, decreased extensibility) due to the formation of physical crosslinks between neighboring chain segments and (2) a change in the chemical potential of the hydrogel due to the decreased ion concentration. A single Ca^{2+} ion is expected to form complexes with 2 COO^- groups while a single Al^{3+} ion can form complexes with 3 COO^- groups. Prior work by Horkay, *et al.*[26] has found that Ca^{2+} ions were delocalized within the polymer networks of swollen hydrogels and were believed to promote aggregation of individual polymer chain segments into loose bundles. This aggregation may restrict the motion of the polymer segments somewhat but was observed to not directly affect the elastic modulus of the hydrogel; any change in the elastic modulus was only a function of the degree of swelling.[26] Thus, the ionic crosslinks formed by Ca^{2+} are considered to be relatively weak physical crosslinks. It is expected that stronger, localized ionic crosslinks are formed between trivalent Al^{3+} and anionic groups in the polymer network, as previous work has shown that rare earth cations (La^{3+} and Ce^{3+}) bind irreversibly to polyacrylate polymer network, causing permanent de-swelling of the hydrogels.[54] The implications of these "weak" Ca^{2+} and "strong" Al^{3+} ionic crosslinks in the PANa-PAM hydrogel samples will be explored further in Section 4.2. with characterization of the samples' mechanical properties.

4.1.3 Effect of PANa-PAM Hydrogel Sample Size

In all previously described results, PANa-PAM hydrogel samples were composed of particles of size 425-850 µm. To determine the effect of the chosen size range on the swelling behavior and ionic sensitivity, hydrogel samples composed of 106-425 µm particles were created and characterized. Both particle size ranges are compared in Figure 13, which displays the swelling curves for 17 wt.% and 83 wt.% PANa concentration PANa-PAM hydrogel samples in pure water and Ca^{2+} solutions. The measured equilibrium swelling ratios were found to be independent of particle size. As expected, the swelling rate was faster for the smaller hydrogel particles. It required 2 minutes for the 106-425 µm particles to reach its maximum swelling ratio but approximately 10-15 minutes for the 425-850 µm particles to reach their maximum swelling ratio.

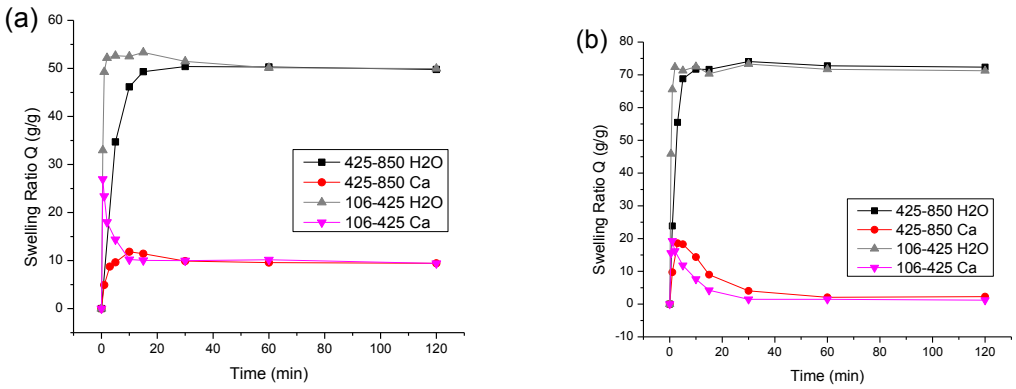

Figure 13. The transient swelling response as a function of sample size (106-425 µm, 425-850 µm) and immersion solution (pure water, Ca^{2+}) for two different hydrogel compositions: (a) 17 wt.% PANa-PAM hydrogel sample, 2 wt.% covalent crosslinking density and (b) 83 wt.% PANa-PAM hydrogel sample, 2 wt.% covalent crosslinking density.

Discussion

The size of SAP particles has important implications for the real-world application in concrete. Jensen and Hansen[2] showed that small SAP particles (a few µm across) may show a decreased absorbency due to less active surface zone compared to the bulk. Esteves [23] studied 50-500 µm SAP particles swollen in synthetic pore solution with optical microscopy and he showed that SAP particle's size will both affect the absorbency and swelling rate of SAP. The absorbency of SAP increased slightly from 13 ml/g to 15.5 ml/g as the particle size increased from 113µm to 488µm. But in the present study, no significant absorbency difference was observed for the two investigated particle size ranges, most likely because the two selected samples with different size ranges are relatively large (> 100 µm) which are beyond the "small"

particles suggested by Jensen. Also the absorbency reported here is the overall absorbency of 0.2g polymers instead of single SAP particles studied by Esteves.

As shown in Figure 13, the particle size had a very strong effect on the swelling kinetics of the samples. The observed increase in swelling rate as particle size decreased is consistent with results from Esteves.[23] As swelling is controlled by diffusion of fluid into the hydrogel, the size dependence can be described by Fick's second law, as given by the following equation:

$$\frac{dQ}{dt} = k(Q_{max} - Q) \qquad \text{Eq. 3}$$

where Q_{max} and Q are the swelling capacities at equilibrium and at any time t, and k is the swelling rate constant which depends on the particle size and can be described as $k = (2.76 \times 10^3)\ \Phi^{-1567}$ for particles immersed in synthetic pore solution where Φ represents the diameter of the particle (μm).[23] Thus, as particle size decreases, the swelling rate will increase dramatically, consistent with the trends displayed in Figure 13.

4.2 Characterization of Macroscale Samples

Macroscale (mm-sized) samples of the PANa-PAM hydrogel samples were created and characterized in order to more fully understand the behavior of the hydrogels in multi-

valent ion solutions. As described in Section 4.1.2 (also Table 4), the equilibrium swelling ratio of PANa-PAM gels in Al^{3+} solutions was observed to be greater than in Ca^{2+} solutions for the 67 wt.% and 83 wt.% PANa samples, which was not anticipated. Additionally, the samples immersed in Al^{3+} solutions became much stiffer to slight mechanical pressure compared with other samples. To directly quantify the changes in mechanical response, samples with macroscopic dimensions were required in order to use conventional compression testing methods.

While the swelling performance of SAP particles is generally regarded as the most important material property, the mechanical response of the particles must not be overlooked as SAP particles must have sufficient strength and mechanical toughness to withstand the external forces encountered during mixing, pumping, and placement of concrete. For example, low-moduli (soft) SAP particles could be crushed or flattened during processing, severely restricting their swelling performance, whereas high-moduli (stiff) particles could be more likely to fracture into smaller particles.

4.2.1 Swelling Study of Macroscale Samples

Figure 14a displays the transient swelling behavior of macroscale hydrogel samples in Ca^{2+} and Al^{3+} solutions. The equilibrium swelling ratio of 17 wt.% PANa samples in Al^{3+} solutions was smaller than in Ca^{2+} solutions while the equilibrium swelling ratio of 67 wt.%

PANa samples in Al^{3+} solutions was greater than results from the Ca^{2+} solutions. This trend is consistent with the swelling behavior of the 425-850µm samples reported in Table 4, though the exact equilibrium values of the macroscale samples differ somewhat. The 17 wt.% PANa sample in Ca^{2+} did not display a peak in the swelling response but did display a broad peak during immersion in the Al^{3+} solution. The 67 wt.% PANa sample displayed narrow peaks in both solutions.

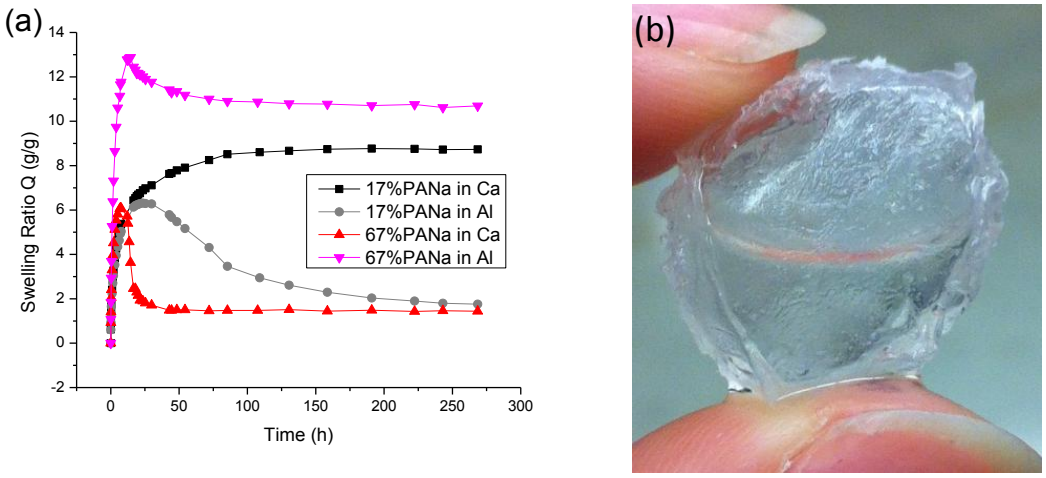

Figure 14. (a) Absorption of macroscale PANa-PAM hydrogel samples with 1 wt.% covalent crosslinking density in Ca^{2+} and Al^{3+} solutions. (b) Photograph of a macroscale PANa-PAM hydrogel sample (67 wt.% PANa, 1 wt.% covalent crosslinking density) following immersion in Al^{3+} solution after reached swelling equilibrium.

The physical characteristics of the macroscale PANa-PAM hydrogel samples swollen to equilibrium in Ca^{2+} or Al^{3+} were very different. The samples immersed in Ca^{2+} solutions appeared to be more elastic and tougher compared to samples immersed in pure water which were easily broken by applying small compressive forces (*e.g.*, by touching with

finger). The samples with 17 wt.% PANa concentration immersed in Al^{3+} solutions displayed an even greater increase in elasticity and toughness (behaving more like a hard rubber than a conventional gel) than similar sample immersed in Ca^{2+} solutions. Surprisingly, the 67 wt.% and 83 wt.% PANa hydrogel samples immersed in Al^{3+} solutions formed a stiff, solid-like shell. This shell started to form after 1.5 hours of immersion in the solution. After the PANa-PAM hydrogel sample reached swelling equilibrium, a complete "core-shell" structure formed and was strong enough to successfully retain fluid within the core of the sample, as shown in Figure 14b. When the sample was carefully sectioned, the fluid-filled core was observed to be mechanically soft and the stiff outer shell could be removed from the sample (note: mechanical tests of the isolated shell are reported in Section 4.2.2). In the present study, 33 wt.% PANa macroscale samples immersed in Al^{3+} solutions were also studied and this system was not observed to form the core-shell structure.

Discussion

As described in Section 4.1.2, the formation of ionic crosslinks is believed to lead to a reduction in the equilibrium swelling ratio. This was directly apparent for PANa-PAM hydrogel samples immersed in Ca^{2+} solutions or PANa-PAM hydrogels containing a low concentration of anionic groups (17 wt.% and 33 wt.%) in Al^{3+} solutions.

The main experimental result observed here was the formation of a soft-core/stiff-shell structure of the macroscale hydrogel samples containing >33 wt.% PANa during immersion in Al^{3+} solutions. This core-shell structure directly impacted the swelling response (see Figure 14a) of the hydrogel samples. The stiff shell was believed to be formed by a high density of Al^{3+}-facilitated ionic crosslinks within the outer region of the hydrogel sample. Such an ionic "barrier" appeared to hinder fluid release from the hydrogel sample, explaining the increased equilibrium swelling ratio for 67 wt.% and 83 wt.% PANa samples immersed in Al^{3+} solutions compared with similar samples immersed in the Ca^{2+} solutions (see Figure 14a and Table 4).

It appears that ionic crosslinks formed by divalent ions (Ca^{2+}) only displayed one effect on the equilibrium swelling ratio (*i.e.*, ratio reduction due to network chain retraction), while the ionic crosslinks formed by trivalent ions (Al^{3+}) displayed *two* competing effects on the equilibrium swelling ratio of PANa-PAM hydrogels: (1) network chain retraction, due to the formation of ionic crosslinks within the network, resulting in the release of fluid; (2) hindered fluid transport, due to the high density of ionic crosslinks that can form in the outer regions of the sample, resulting in a stiff surface shell. For low-concentration PANa samples immersed in Al^{3+} solutions, effect (1) was dominant and the equilibrium swelling ratio decreased. For high-concentration PANa samples immersed in Al^{3+} solutions, effect (2) was dominant and the equilibrium swelling ratio

increased. This result indicated that in addition to the valency of ions contained in the swelling fluid, the swelling performance and fluid release rate of the PANa-PAM hydrogel samples was strongly dependent on the concentration of anionic groups within the polymer network which contribute in ionic crosslinking reactions.

The effect of ion valency on fluid release rate was further verified by the transient swelling response of the PANa-PAM hydrogel sample. The transient swelling response of the 17 wt.% PANa-PAM hydrogel sample immersed in Ca^{2+} did not contain a short-time peak but did display a broad peak when immersed in the Al^{3+} solution (indicating fluid absorption and subsequent release). This was because the ionic crosslinks formed by Al^{3+} were localized in the polymer network compared with the weak and delocalized crosslinks formed by Ca^{2+} and thus the chain retraction forces from the presence of Al^{3+} would be stronger and dominant. This results in fluid release and formation of the broad peak in the transient swelling response. By comparison, the short-time peak for samples containing 67 wt.% PANa immersed in Al^{3+} solutions was very narrow and smaller in magnitude because of hindered fluid transport due to formation of the stiff outer shell which slowed/prevented fluid release. The stronger ionic crosslinks formed by Al^{3+} is the reason for the increased equilibrium swelling ratios for 67 wt.% and 83 wt.% PANa hydrogel samples immersed in Al^{3+} solution compared with samples in Ca^{2+} solution (refer back to Table 4).

Referring back to Figure 10, the short-time swelling peak for samples immersed in Ca^{2+} solutions became narrower as PANa concentration increased. As the amount of ionic crosslinks increased with PANa concentration, the hydrogel samples with greater PANa concentration have an increased tendency to release fluid due to enhanced chain retraction forces which leads to a narrower short-time swelling peak.

4.2.2 Mechanical Test of Macroscale Samples

To further investigate the properties of the macroscale PANa-PAM hydrogel samples, compression tests were performed on macroscale samples swollen in different ionic solutions. Figure 15 displays the compressive stress responses for macroscale hydrogel samples with specific swelling ratios in Ca^{2+} solutions. The calculated elastic moduli of the samples are reported in Table 4. The elastic modulus for the samples with 2 wt.% covalent crosslinking density were much larger than the samples with 1 wt.% density, consistent with rubber elasticity theory (Eq. 2). As shown in Table 4, elasticity was observed to decrease as the swelling ratio increased for the samples with 1 wt.% covalent crosslinking densities while the elasticity of samples containing 2 wt.% covalent crosslinking density appeared to increase with swelling for the two ratio values investigated here. Figure 15 also displays the almost completely overlapping stress responses of the 2 wt.% covalent crosslinking density samples immersed in water and Ca^{2+} solution with identical swelling ratios of ~ 4.3 g/g.

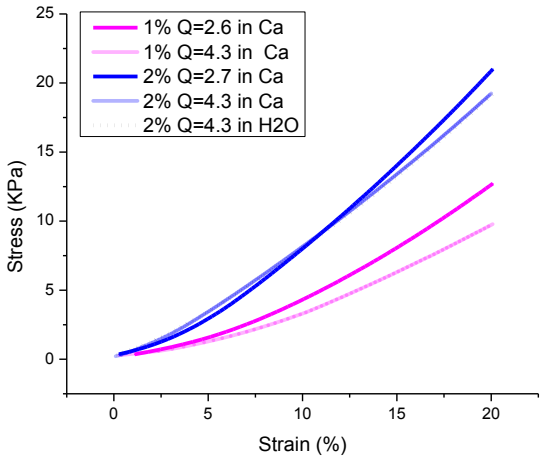

Figure 15. Compressive stress response of macroscale hydrogel samples with 67 wt.% PANa containing 1 or 2 wt.% covalent crosslinking densities and swollen to different Q-ratios in Ca^{2+} and deionized solutions.

Table 5. Elastic moduli of macroscale PANa-PAM hydrogel samples with 67 wt.% PANa containing 1 or 2 wt.% covalent crosslinking density.

Covalent Crosslinking Density	Swelling Ratio, *Q* (g/g)	Elastic Modulus (Ca^{2+} solutions)
1 wt.%	2.6	26.4 KPa
	4.3	14.8 KPa
2 wt.%	2.7	40.5 KPa
	4.3	54.4 KPa

Figure 16 displays the compressive stress responses for macroscale hydrogel samples containing 67 wt.% PANa and 2 wt.% covalent crosslinking density and swelling ratios of around 2.7 g/g in Al^{3+} and Ca^{2+} solutions. The hydrogel sample displayed a much stiffer

stress response following immersion in Al^{3+} solutions than the sample immersed in the Ca^{2+} solutions. Additionally, cracking sounds were heard during compression testing of samples in Al^{3+} solutions. The elastic modulus of the sample immersed in Al^{3+} solution was calculated to be 102.6 KPa, an order of magnitude larger than results obtained for a similar sample immersed in Ca^{2+} solution (40.5 KPa, see Table 5).

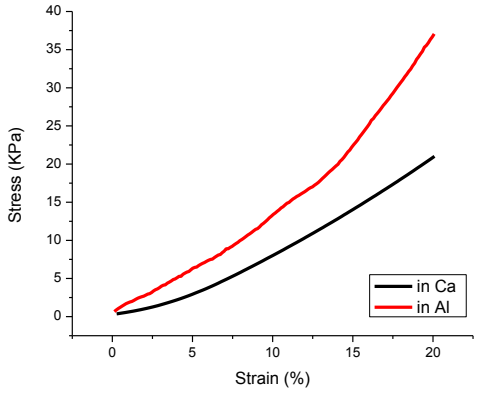

Figure 16. Compressive stress response of macroscale hydrogel samples containing 67 wt.% PANa and 2 wt.% covalent crosslinking density, with swelling ratio of approximately 2.7 g/g in Al^{3+} solutions.

To better understand the mechanical properties of the macroscale hydrogel samples swollen in Al^{3+}, specimens of the stiff outer shell of the hydrogel sample were isolated and tested in tension. Figure 17 displays the tension stress response of the shell specimens after the hydrogel samples reached swelling equilibrium in Al^{3+} solutions. The elastic modulus was calculated to be 59.5 MPa (67 wt.% PANa sample with 1 wt.% covalent crosslinking density), 107.2 MPa (83 wt.% PANa sample with 1 wt.% covalent

crosslinking density) and 125.4 MPa (83 wt.% PANa sample with 2 wt.% covalent crosslinking density). Thus, compared to results in Table 5, the elastic modulus for the stiff outer shells of the PANa-PAM hydrogel samples was approximately 1000 times greater than the overall compression modulus of the core-shell samples and the modulus of similar samples immersed in Ca^{2+} solutions.

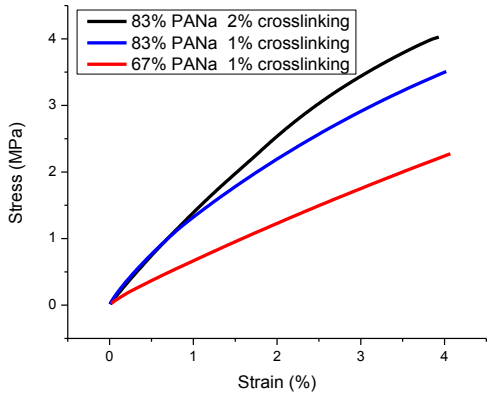

Figure 17. Tensile stress response of specimens of the stiff outer shell of different PANa-PAM hydrogel samples after swelling equilibrium was reached in Al^{3+} solutions.

Discussion

As mentioned in Section 4.1.2, the ionic crosslinks formed by Ca^{2+} ions are relatively weak and delocalized within the network and prior work has found that the aggregation of polymer chains caused by Ca^{2+} ions does not affect the elastic modulus of polymer network.[26] This explained why the compressive stress responses of the 2 wt.% covalent crosslinking density samples immersed in water and Ca^{2+} solution almost perfectly

overlap with each other (shown in Figure 15). Also stated in Section 2.1.4, increased covalent crosslinking density leads to increased elastic modulus (*i.e.*, rubber elasticity theory)[28] which provides rationale for effective doubling of the elastic modulus in Table 5 when the covalent crosslinking density increased from 1 wt.% to 2 wt.% for PANa-PAM hydrogel samples with 67 wt.% PANa immersed in Ca^{2+} solutions.

It was also observed that the equilibrium swelling ratio affected the compressive stress response of PANa-PAM hydrogels immersed in Ca^{2+} solutions, with greater swelling ratios resulting in reduced elastic moduli. The greater volume of water within the hydrogel allows for increased segmental mobility of the polymer chains in the network and subsequently faster relaxation in response to an applied stress. This was confirmed by the reduced elastic modulus of samples with 1 wt.% covalent crosslinking densities (Table 5). However, the opposite trend was observed for samples with 2 wt.% covalent crosslinking densities. This could be due to an imperfection of the particular sample. Equally likely is that for the range of swelling ratios investigated here, the elastic modulus is more strongly dependent the covalent density and more weakly dependent on swelling ratio.

The cracking sound that was observed during mechanical testing of samples swollen in Al^{3+} solutions suggested that the stiff outer shell (seen in Figure 14b) was very hard and

brittle. This stiff shell resulted in the overall stiffer mechanical response that was observed during compression testing of samples equilibrated in Al^{3+} solutions compared with the response of samples equilibrated in Ca^{2+} solutions (see Figure 16). The isolated tensile stress response of specimens of the PANa-PAM hydrogel's outer shell layer further explains the nature of the strong ionic crosslinks formed by Al^{3+}. The elastic modulus of the stiff shells was observed to be in the MPa range. As shown in Figure 17, increased PANa concentration in the hydrogel sample strongly enhanced the shell's stiffness, most likely due to increased density of the Al^{3+} ionic crosslinks in the outer region of the sample facilitated by the greater overall concentration of anionic groups in the polymer network of the high-concentration PANa hydrogel samples. By comparison, only weak enhancement of the shell's stiffness was observed with an increase in covalent crosslinking density from 1 wt.% to 2 wt.% (Figure 17). Thus, the enhanced mechanical properties of the PANa-PAM hydrogel samples were primarily a result of the presence of Al^{3+} and the subsequent formation of a strong, ionic crosslinked, core-shell structure.

4.3 Swelling Study in Synthetic Pore Solution

Figure 18 shows the swelling ratio for PANa-PAM samples containing different concentrations of PANa in synthetic pore solution. The shape of the curves is very similar to those obtained from water or Na^{+} solutions. After a quick initial intake of fluid

the swelling ratio reached a plateau except for 17 wt.% PANa sample of which the swelling ratio increased slowly after the quick intake of fluid during the observation period. The equilibrium swelling ratio of 17 wt.% and 67 wt.% PANa samples were 13.0g/g and 15.9g/g which were very closed to the values (11.5g/g for 17 wt.% PANa sample and 16.0 wt.% for 67 wt.% PANa sample) obtained from real pore solutions using 45-106μm particles. Also, as the PANa concentration increased from 17 wt.% to 67 wt.%, the swelling ratio increased and then decreased slightly as the PANa concentration increased further to 83 wt.%. However, no obvious ionic crust was observed in all the samples swollen in synthetic pore solution or real pore solution.

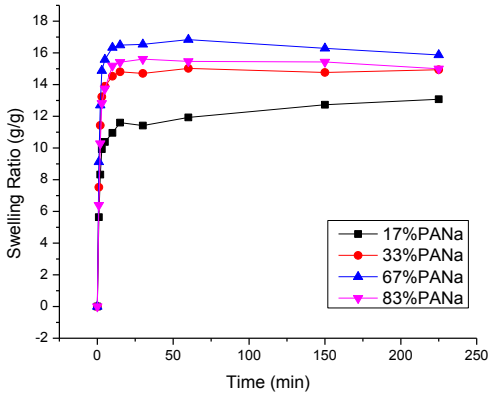

Figure 18. Absorption of 45-106μm PANa-PAM hydrogel samples with 2 wt.% covalent crosslinking density in synthetic pore solutions.

Discussion

The swelling capacity and kinetics of PANa-PAM hydrogels in the synthetic pore solution was different from that in multi-valent ion solutions (Ca^{2+} or Al^{3+}, Figure 10 and Figure 11) but very similar to that in mono-valent ion solutions (Na^{+}, Figure 8). This was expected due to the much higher concentration of mono-valent ions (801 mM) than multi-valent ions (5.4 mM) in the synthetic pore solution. In such solution, the effect of ionic crosslinks formed by Ca^{2+} or Al^{3+} and COO^{-} groups in PANa-PAM hydrogels may not lead to an obvious decrease of swelling ratio or formation of the stiff ionic shells.

Same as we stated before, the equilibrium swelling ratio of PANa-PAM hydrogels increased as the PANa concentration increased from 17 wt.% to 67 wt.% due to a higher osmotic pressure which originates from higher PANa concentration. However, the equilibrium swelling ratio decreased slightly from 15.8 g/g to 15 g/g as PANa concentration increased further from 67 wt.% to 83 wt.%. This most likely resulted from an increased concentration of ionic crosslinks that form in 83 wt.% PANa sample than compared to the other samples. This would result in network chain retraction and reduce the overall absorption capacity of the 83 wt.% PANa hydrogel. While for other samples, the ionic crosslinks formed in the polymer network may be too weak to affect the equilibrium swelling ratio.

Another explanation of the slightly decrease of equilibrium swelling ratio as PANa concentration increased from 67 wt.% to 83 wt.% is that not all –COONa groups along the polymer chains dissociate to form $–COO^-$ groups and free Na^+ ions. As a result, the concentration of $–COO^-$ groups is lower than we expected. Referring to Figure 8, the similar result can be found. The equilibrium swelling ratio of PANa-PAM gels did not increase further in Na^+ solutions as the PANa concentration increased from 67 wt.% to 83 wt.%. However, this theory might be more suitable to explain why no further increase of equilibrium swelling was observed as PANa concentration increased above 67 wt.%. A similar result was found by Yarimkaya[8] who offered another reason for decreased swelling ratio as the concentration of $–COO^-$ groups increased. They believed that the low molecular weight polymeric chains were obtained as the polymerization rate was too fast due to increased amount of carboxylate groups.

Ultimately, we believe that the ionic crosslinking which was formed by Ca^{2+} or Al^{3+} and COO- groups has the major influence on the decreased equilibrium swelling ratio observed in Figure 18 as PANa concentration increased from 67 wt.% to 83 wt.%.

4.4 Internal Humidity of Mortar With and Without SAP

The internal relative humidity of casted mortar with and without SAP was monitored. The mortar specimens were cast into airtight containers and allowed to hydrate for 2

days. After this period, the samples were crushed and placed in the Rotronic cells. Figure 19 reports the internal relative during 69-103 hour period. It is noticed that the relative humidity of plain mortar sample dropped to 87% after 70 hours and continued to drop to 85% after 100 hours. While the relative humidity of mortar sample with ether SAP I(17 wt.% PANa) or SAP II(67 wt.% PANa) was much higher than that of the plain mortar.

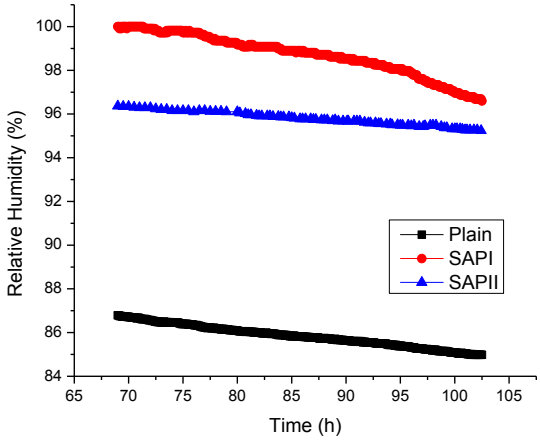

Figure 19. Relative humidity in setting mortar samples with and without SAP.

Discussion

Figure 19 shows that the addition of SAP I or SAP II was effective to keep the internal relative humidity of mortar samples higher than the plain sample. At the beginning of mortar casting, the chemical shrinkage of mortar mixture could be transformed into external bulk volume change. As the mortar hardened, the free water was consumed

and empty pores were formed inside the mortar. The relative humidity dropped subsequently. The incorporated SAP appeared to serve as an internal water supply which released free water back to the mortar system and helped keep the relative humidity at a high value (above 95% for SAP I and SAP II).

4.5 Autogenous Shrinkage of Mortar With and Without SAP

Figure 20 shows the autogenous shrinkage of plain mortar sample and mortar with SAP after setting for 9 days. The autogenous deformations are zeroed at 5 hours (time of set) after placing the corrugated tubes in the temperature constant room when solid skeleton started to form in the mortar. A considerable shrinkage can be found in plain mortar and the autogenous shrinkage reached 330 microstrain after 9 days. Compared to the plain mortar, both SAP I and SAP II decreased the autogenous shrinkage to a large extent. Mortar sample with SAP II exhibited a small expansion after setting. In the present work, we found the SAP I and SAP II were effective through the whole observation period as shown in Figure 20 and only after the initial slight shrinkage the mortar sample barely shrank any further.

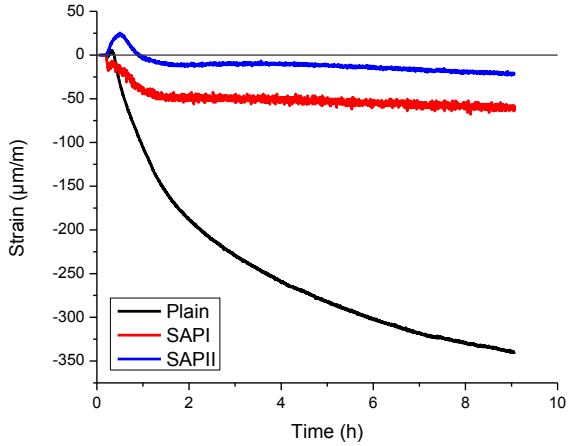

Figure 20: Autogenous deformation of mortar with and without SAP, w/c=0.3.

Discussion

Both SAP I and SAP II had a strong effect on decreasing the autogenous shrinkage of mortar which was due to the constant water supply during mortar setting offered by SAP. The gradually released water from SAP to mortar system helped mitigate the self-desiccation which happened after free water was depleted in plain mortar sample. The reason of the small expansion observed right after the setting in mortar sample with SAP II is not fully understood yet. The same findings was reported by Schröfl[3] and they proposed that the addition of SAP may modify the formation of portlandite which is the reason for early stage expansion. Also they suggested that ettringite crystallization should be taken into consideration.

The reason that SAP II is more effective than SAP I for decreasing the autogenous shrinkage could be that more free water was released from SAP II after setting. Without further experiments, we provide several explanations here for why more water could be released from SAP II.

First, although the amount of SAP was calculated based on its equilibrium swelling ratio in real pore solution, it is possible that SAP may not reach its equilibrium swelling ratio in the mortar mixture. The equilibrium swelling ratio of SAP was collected from non-stirred solution and the pore solution was a greater volume (50ml pore solution was used for 0.2g SAP) than what was needed for SAP to reach its equilibrium swelling ratio. However, SAP added in mortar mixture had to absorb fluid from cement paste during mixing so it is possible that exactly amount of water absorbed by SAP deviated from the designed 0.5 bwoc (by weight of cement). Referring to Figure 7 and Figure 8, PANa-PAM hydrogels containing higher amount of PANa displayed faster initial swelling rate and bigger equilibrium swelling ratio. Since SAP II (67 wt.% PANa) has a higher PANa concentration than SAP I (17 wt.% PANa), SAP II has stronger ability to compete for water than SAP I during the first few minutes of cement mixing. So that SAP II could absorb more water during the mixing than SAP I and that makes sense for more water released from SAP II than SAP I.

The second explanation offered here takes the desorption ability of SAP into consideration. Given the assumption that both SAP I and SAP II would absorb the same amount of expected water, the desorption ability of SAP II might be stronger than SAP I which leads to a larger amount of water released back to mortar samples. We believe that there is connection between the chemical structure of SAP particles and desorption behavior although it is not studied in the present work.

Another factor that needs discussion is the gel-blocking effect which is only taken into account for particles smaller than 100μm.[14] Gel blocking usually refers to the phenomenon that extensive swollen SAP particles cause closure of capillary pores which prevents further fluid absorption.[59] The SAP we used in mortar was 45-106μm and the gel-blocking effect might happen which would decrease the amount of fluid absorbed in SAP. The equilibrium swelling ratio of SAP II (16.5 g/g) is bigger than SAP I (11.5 g/g) so that smaller amount of SAP II than SAP I was required for additional 0.5 bwoc free water added in mortar. More SAP I particles were added into mortar which leaves a higher chance for gel-blocking phenomenon to happen. As a result, the total amount of fluid absorbed by SAP I could be less than SAP II.

After the initial stage, the two strain-time curves of SAP I and SAP II were almost paralleled which suggests that desorption behavior of SAP I and SAP II was similar during

that period. However, during this period, the slope of strain-time curve of mortar with SAP was smaller than that of plain mortar which suggests that the SAP continued to serve as an internal water reservoir during the whole observation period.

CHAPTER 5. CONCLUSIONS AND FUTURE WORK

5.1 Summary and Main Conclusions

The effect of ions on the swelling and mechanical properties of model SAP hydrogels was characterized here, using a series of poly(sodium acrylate-acrylamide) (PANa-PAM) random copolymer networks with varying concentrations of PANa. By synthesizing the hydrogels in-house, samples with independently tunable amounts of covalent crosslinking and anionic functional groups were created, allowing for the effects of covalent and ionic crosslinking on the properties of the hydrogels to be separately quantified. Free swelling experiments were performed with PANa-PAM hydrogel samples with four particle sizes (45-106 μm, 106-425 μm, 425-850 μm, and mm-sized "macroscale" samples). For the experiments, the swelling capacity and kinetics were characterized during sample immersion in deionized water and Na^{+}, Ca^{2+}, and Al^{3+} solutions. Mechanical tests were also performed on the macroscale samples following equilibration in the different solutions. Finally two PANa-PAM gels with 17 wt.% and 67 wt.% PANa concentration were added into mortar and their effect on internal relative humidity and autogenous shrinkage was studied. The main experimental outcomes were the following:

1) The swelling capacity and kinetics of PANa-PAM hydrogels was strongly sensitive to the presence of ions in solution. For hydrogel samples containing a relatively low concentration of PANa (17, 33 wt.%), the equilibrium swelling ratio decreased in the following fashion: Q(water) > Q(Na^+) > Q(Ca^{2+}) > Q(Al^{3+}). For hydrogel samples containing a relatively high concentration of PANa (67, 83 wt.%), the equilibrium swelling ratio decreased in the following fashion: Q(water) > Q(Na^+) > Q(Al^{3+}) > Q(Ca^{2+}). The presence of ions caused rapid swelling and de-swelling of the samples to occur.

2) Increased covalent crosslinking density in the PANa-PAM hydrogel samples resulted in a decreased equilibrium swelling ratio for samples immersed in water or Na^+ solutions, consistent with theories from rubber elasticity. However in the presence of ions, the swelling performance of the hydrogels became less sensitive to covalent crosslinking density.

3) Compression testing of samples immersed in Ca^{2+} solutions indicated that greater swelling ratio or reduced covalent crosslinking density resulted in hydrogels with reduced elastic modulus (~ kPa), again consistent with rubber elasticity theories. More importantly, the stress response of samples immersed in Ca^{2+} was found to be almost identical to the response of samples immersed in pure water at equivalent Q-values,

indicating that the ionic crosslinks formed by Ca^{2+} ions had no significant impact on the mechanical properties of the samples.

4) For hydrogel samples with high PANa concentration (67 wt.% or 83 wt.%), formation of a mechanically stiff layer at the hydrogel's surface was observed during immersion in Al^{3+} solutions. This stiff "shell" displayed elastic moduli of *O*(100 MPa), which caused the overall elastic modulus of the hydrogel to increase and also prevented the release of fluid from the hydrogel. This effect was not observed during immersion in the Ca^{2+} solutions.

5) The PANa-PAM hydrogels containing both 17 wt.% and 67 wt.% PANa were found to be effective on keeping internal relative humidity high and decreasing autogenous shrinkage of mortar. And PANa-PAM hydrogel with 67 wt.% PANa decreased the autogenous shrinkage better than 17 wt.% PANa sample which suggests there is relationship between the chemical structure of SAP and the performance on decreasing autogenous shrinkage in concrete, although this relationship is not fully understood in the present work.

Overall, the swelling performance, swelling kinetics, and mechanical properties of PANa-PAM hydrogels were found to be strongly dependent on the concentration of anionic

groups in the polymer network and the valency of the ions in the swelling media. The results described here have the following implications. First, by informed selection of the concentration of anionic groups within the polymer network of a SAP particle, it is possible to control the maximum swelling ratio and initial swelling rate, which could be used to create customized SAP particles designed for specific cementing environments. Second, the results presented here may be useful for the development of predictive models that capture the behavior of SAP particles in concrete. With only prior knowledge of the expected concentration and valency of ions in the pore fluid, such models would allow for quantitative predictions of the concentration of anionic groups in the polymer network that would be required to create SAP particles with a desired swelling capacity, fluid release rate, and mechanical response.

5.2 Future Work

As discussed in Session 4.5, the reason why SAP II (67 wt.% PANa) had a better performance on decreasing autogenous shrinkage of mortar than SAP I (17 wt.% PANa) is not clarified. To address this, the relations of the chemical structure of PANa-PAM hydrogel and its desorption behavior in different swelling media should be studied further. Also the amount of water absorbed by SAP during mixing could be studied by comparing the swollen volume of SAP particles in free solution and in concrete mixture using optical microscopy in order to obtain the accurate swelling ratio of SAP.

The ionic shell formed by Al^{3+} and PANa-PAM found in 0.025M Al^{3+} was not observed in the synthetic pore solution (containing 0.0032M Al^{3+}) and this finding suggests that the formation of the ionic shell not only depends on the PANa concentration of the PANa-PAM gels but also depends on the concentration of swelling media (Al^{3+} solution). The relationship of the formation of ionic shell and the concentration of Al^{3+} needs to be studied since the amount of Al^{3+} varies from cement to cement. Whether or not the ionic shells will form in a lower Al^{3+} concentration solution than 0.025M and prevent fluid release needs to be answered. And how the ionic shells may interact with other cementitious materials should be studied. Another reason that more attention should be paid to the ionic shells is that, even if not distinct ionic shells may form by SAP in concrete, the fluid hindered effect of the ionic shell would greatly affect the desorption behavior of SAP. Based on that, we might be able to tune desorption behavior of SAP by adding or eliminating Al^{3+} from cement.

In the present work, the SAP particles were added into cement particles in dry state. In order to find out the optimal procedure to include SAP particles in concrete, swollen SAP particles could be used instead of dry particles. In that case, the amount of extra water trapped by SAP particles can be controlled exactly since SAP particles do not have to compete for water during mixing. And the state of SAP particles after mixing should be studied since the mechanical force during the mixing could crush SAP particles.

LIST OF REFERENCES

LIST OF REFERENCES

1. Jensen, O. M. & Hansen, P. F. Water-entrained cement-based materials I. Principles and theoretical background. *Cem. Concr. Res.* **31,** 647–654 (2001).

2. Jensen, O. M. & Hansen, P. F. Water-entrained cement-based materials II. Experimental observations. *Cem. Concr. Res.* **32,** 973–978 (2002).

3. Schröfl, C., Mechtcherine, V. & Gorges, M. Relation between the molecular structure and the efficiency of superabsorbent polymers (SAP) as concrete admixture to mitigate autogenous shrinkage. *Cem. Concr. Res.* **42,** 865–873 (2012).

4. Craeye, B., Geirnaert, M. & Schutter, G. De. Superabsorbing polymers as an internal curing agent for mitigation of early-age cracking of high-performance concrete bridge decks. *Constr. Build. Mater.* **25,** 1–13 (2011).

5. Laura, P., Durand, F. & Jensen, O. Autogenous strain of cement pastes with superabsorbent polymers. in *Proc. internaltional RILEM Conf. Vol. Chang. Hardening Concr. Test. Mitig.* (Jensen, O., Laura, P. & K, K.) 57–66 (2006).

6. Murali Mohan, Y., Keshava Murthy, P. S. & Mohana Raju, K. Preparation and swelling behavior of macroporous poly(acrylamide-co-sodium methacrylate) superabsorbent hydrogels. *J. Appl. Polym. Sci.* **101,** 3202–3214 (2006).

7. Yarimkaya, S. & Basan, H. Synthesis and Swelling Behavior of Acrylate-Based Hydrogels. *J. Macromol. Sci. Part A* **44,** 699–706 (2007).

8. Chen, X.-P., Shan, G.-R., Huang, J., Huang, Z.-M. & Weng, Z.-X. Synthesis and properties of acrylic-based superabsorbent. *J. Appl. Polym. Sci.* **92,** 619–624 (2004).

9. Bahaj, H., Benaddi, R., Bakass, M. & Bayane, C. Swelling of Superabsorbents Polymers in an Aqueous Medium. *J. Appl. Polym. Sci.* **115,** 2479–2484 (2010).

10. Raju, K. M., Raju, M. P. & Mohan, Y. M. Synthesis of superabsorbent copolymers as water manageable materials. *Polym. Int.* **52,** 768–772 (2003).

11. Siriwatwechakul, W., Siramanont, J. & Vichit-Vadakan, W. Behavior of Superabsorbent Polymers in Calcium- and Sodium-Rich Solutions. *J. Mater. Civ. Eng.* **24,** 976–980 (2012).

12. Zhu, Q., Christopher, B. W. & Erk, K. A. Effect of ionic crosslinking on the swelling and mechanical response of model superabsorbent polymer hydrogels for internally cured concrete. *Mater. Struct.* Accpeted: 8 April 2014.

13. Andersson, K., Allard, B., Bengtsson, M. & Magnusson, B. Chemical composition of cement pore solutions. *Cem. Concr. Res.* **19,** 327–332 (1989).

14. Friedrich, S. in *Appl. Super Absorbent Polym. Concr. Constr.* (Mechtcherine, V. & Reinhardt, H.-W.) 13–18 (Springer Netherlands, 2012). doi:10.1007/978-94-007-2733-5

15. Buchholz, F. L. in *Mod. Superabsorben Polym. Technol.* 251–269 (1998).

16. Staples, Thomas L.;Henton, David E.;Buchhol, F. L. in *Mod. Superabsorben Polym. Technol.* 19–20 (1988).

17. Buchholz, F. L. in *Mod. superabsorbent Polym. Technol.* (Buchholz, F. L. & Graham, A. T.) 1–18 (John Wiley & Sons, 1998).

18. Jar, P.-Y. B. & Wu, Y. S. Effect of counter-ions on swelling and shrinkage of polyacrylamide-based ionic gels. *Polymer (Guildf).* **38,** 2557–2560 (1997).

19. Nakason, C., Wohmang, T., Kaesaman, A. & Kiatkamjornwong, S. Preparation of cassava starch-graft-polyacrylamide superabsorbents and associated composites by reactive blending. *Carbohydr. Polym.* **81,** 348–357 (2010).

20. Zhang, Y., Wang, L., Li, X. & He, P. Salt-resistant superabsorbents from inverse-suspension polymerization of PEG methacrylate, acryamide and partially neutralized acrylic acid. *J. Polym. Res.* **18,** 157–161 (2010).

21. Chen, Z., Liu, M. & Ma, S. Synthesis and modification of salt-resistant superabsorbent polymers. *React. Funct. Polym.* **62,** 85–92 (2005).

22. Siriwatwechakul, W., Siramanont, J. & Vichit-Vadakan, W. Superabsorbent polymer structures. in *Int. RILEM Conf. Use Superabsorbent Polym. Other New Addit. Concr.* 253–262 (2010).

23. Esteves, L. P. Superabsorbent polymers: On their interaction with water and pore fluid. *Cem. Concr. Compos.* **33,** 717–724 (2011).

24. Kabiri, K., Zohuriaan-Mehr, M. J., Bouhendi, H., Jamshidi, A. & Ahmad-Khanbeigi, F. Residual monomer in superabsorbent polymers: Effects of the initiating system. *J. Appl. Polym. Sci.* **114,** 2533–2540 (2009).

25. Liu, Z. & Rempel, G. Preparation of superabsorbent polymers by crosslinking acrylic acid and acrylamide copolymers. *J. Appl. Polym. Sci.* **64,** 1345–1353 (1997).

26. Horkay, F., Tasaki, I. & Basser, P. J. Osmotic swelling of polyacrylate hydrogels in physiological salt solutions. *Biomacromolecules* **1,** 84–90 (2000).

27. Buchholz, F. L. in *Superabsorbent Polym.* 27–38 (1994). doi:10.1021/bk-1994-0573.ch002

28. Rubinstein, M. & Colby, R. H. *Polymer Physics*. (OUP Oxford, 2003).

29. Henderson, K. J., Zhou, T. C., Otim, K. J. & Shull, K. R. Ionically Cross-Linked Triblock Copolymer Hydrogels with High Strength. *Macromolecules* **43,** 6193–6201 (2010).

30. Breitenbücher, R. Developments and applications of high-performance concrete. *Mater. Struct.* **31,** 209–215 (1998).

31. Weiss, W. J., Yang, W. & Shah, S. P. Shrinkage Cracking of Restrained Concrete Slabs. *J. Eng. Mech.* **124,** 765–774 (1998).

32. Lura, P., Jensen, O. & Breugel, K. van. Autogenous shrinkage in high-performance cement paste: An evaluation of basic mechanisms. *Cem. Concr. Res.* **33,** 223–232 (2003).

33. Geiker, M. R., Bentz, D. P. & Jensen, O. M. in *High-Performance Struct. Light. Concr.* 143–148 (2004).

34. Hammer, T. High strength LWA concrete with silica fume—Effect of water content in the LWA on mechanical properties. in *Suppl. Pap. 4th CANMET/ACI Int. Conf. Fly Ash, Silica Fume, Slag Nat. Pozzolans Concr. Istanbul, Turkey,* 314–330 (1992).

35. *RILEM Report 41 Internal Curing of Concrete – State of the Art Report of TC 1966-IC*. 140 (Springer, 2007).

36. Streeter, D. A., Wolfe, W. H. & Vaughn, R. E. in *ACI SP 290* (Schindler, A., Grygar, G. & Weiss, W. J.) (2012).

37. Di Bella, C., Villani, C., Phares, N., Hausheer, E. & Weiss, W. J. Chloride Transport and Service Life in Internally Cured Concrete. in *Am. Soc. Civ. Eng. Struct. Congr.* (2012).

38. Schlitter, J., Henkensiefken, R., Castro, J., Raoufi, K. & Weiss, W. J. *Development of Internally Cured Concrete for Increased Service Life - FHWA/IN/JTRP-2010/10*. (2010).

39. Di Bella, C., Schlitter, J., Carboouneau, N. & Weiss, W. J. *Documenting the Construction of a Plain Concrete Bridge Deck and an Internally Cured Bridge Deck - Joint Transportation Research Program*. (2012).

40. Guthrie, W. S. & Yaede, J. M. *Internal Curing of Concrete Bridge Decks in Utah: Preliminary Evaluation - Transportation Research Board*. 17 (2013).

41. Bentur, A., Igarashi, S. & Kovler, K. Prevention of autogenous shrinkage in high-strength concrete by internal curing using wet lightweight aggregates. *Cem. Concr. Res.* **31,** 1587–1591 (2001).

42. Cusson, D. & Hoogeveen, T. Internal curing of high-performance concrete with pre-soaked fine lightweight aggregate for prevention of autogenous shrinkage cracking. *Cem. Concr. Res.* **38,** 757–765 (2008).

43. Bentz, D. & Halleck, P. Water movement during internal curing: Direct observation using x-ray microtomography. *Concr. Internaltional* **28,** 39–45 (2006).

44. Schlitter, J. L., Bentz, D. & Weiss, W. Quantifying Stress Development and Remaining Stress Capacity in Restrained, Internally Cured Mortars. *ACI Mater. J.* **110,** 3–12 (2013).

45. Siramanont, J., Vichit-Vadakan, W. & Siriwatwechakul, W. The impact of SAP structure on the effectiveness of internal curing. in *Int. RILEM Conf. Use superabsorbent Polym. other new Addit. Concr.* (Jensen, O. M., Hasholt, M. T. & Laustsen, S.) 243–252 (RILEM, 2010).

46. Justs, J., Wyrzykowski, M., Winnefeld, F., Bajare, D. & Lura, P. Influence of superabsorbent polymers on hydration of cement pastes with low water-to-binder ratio. *J. Therm. Anal. Calorim.* **115,** 425–432 (2013).

47. Esteves, L. P. On the hydration of water-entrained cement–silica systems: Combined SEM, XRD and thermal analysis in cement pastes. *Thermochim. Acta* **518,** 27–35 (2011).

48. Hasholt, M. T., Jensen, O. M., Kovler, K. & Zhutovsky, S. Can superabsorent polymers mitigate autogenous shrinkage of internally cured concrete without compromising the strength? *Constr. Build. Mater.* **31,** 226–230 (2012).

49. Reinhardt, H. W., Assman, A. & Monning, S. Superabsorbent polymers (SAP) – An Admixture to Increase the Durability of Concrete. in *Int. Conf. Microstruct. Relat. Durab. Cem. Compos.* (Sun, W., van Breugel, K., Miao, C., Ye, G. & Chen, H.) 313–322 (2008).

50. Jones, W. Freeze-Thaw Behavior of Internally Cured Concrete. (2013). Purdue University, West Lafayette.

51. Wyrzykowski, M. & Lura, P. Controlling the coefficient of thermal expansion of cementitious materials – A new application for superabsorbent polymers. *Cem. Concr. Compos.* **35,** 49–58 (2013).

52. Snoeck, D., Van Tittelboom, K., Steuperaert, S., Dubruel, P. & De Belie, N. Self-healing cementitious materials by the combination of microfibres and superabsorbent polymers. *J. Intell. Mater. Syst. Struct.* **25,** 13–24 (2012).

53. Double, D. D., Hewlett, P. C., Sing, K. S. W. & Raffle, J. F. New Developments in Understanding the Chemistry of Cement Hydration [and Discussion]. *Philos. Trans. R. Soc. A Math. Phys. Eng. Sci.* **310,** 53–66 (1983).

54. Horkay, F., Tasaki, I. & Basser, P. J. Effect of monovalent-divalent cation exchange on the swelling of polyacrylate hydrogels in physiological salt solutions. *Biomacromolecules* **2,** 195–9 (2001).

55. Castro, J., Lura, P., Rajabipour, F., Henkensiefken, R. & Weiss, J. Internal Curing : Discussion of the Role of Pore Solution on Relative Humidity Measurements and Desorption of Lightweight Aggregate (LWA). *ACI Special Publication.* **270**, 89–100(2010). doi: 10.14359/51663741

56. Christian, G. D. *Analytical Chemistry*. 742–744 (Wiley, 2004).

57. Cabinets, M. & Rooms, M. Standard Practice for Mechanical Mixing of Hydraulic Cement Pastes and Mortars. 13–15 (2014). doi:10.1520/C0305-13.2

58. Mass, D. & Cements, W. Standard Test Method for Autogenous Strain of Cement Paste and Mortar 1. 1–8 (2013). doi:10.1520/C1698-09.2

59. Co, N. I. & Carolina, N. *ABSORBENT TECHNOLOGY*. 274 (Elsevier, 2002).